AM. IND. HYG. ASSOC. J. 53(9):548-555 (1992)

RESPIRATOR PERFORMANCE RATING TABLES FOR NONTEMPERATE ENVIRONMENTS*

Arthur T. Johnson[a]
Corey M. Grove[b]
Ronald A. Weiss[b]

[a]Agricultural Engineering Department, University of Maryland, College Park, MD 20742-5711; [b]CRDEC, Individual Protection Division, Aberdeen Proving Ground, MD 21010-5423

Respirator performance rating tables have been constructed for hot, humid (29°C, 95% RH); hot, dry (49°C, 30% RH); and cold, dry (-32°C, 70% RH) conditions. These tables convey expected wearer performance percentages compared to unmasked workers for various mask elements and work rates. The hot, humid condition was found to be the most severe overall. Many table entries approach 100%, thus leading to difficulties in correcting mask deficiencies.

The respirator performance rating table (PRT) concept was introduced to assist the design and evaluation of respiratory protective masks and as a first step toward computer-aided mask design. The PRT compares effects of various mask factors on task performance of an individual wearing a mask compared to the unmasked condition. The PRT organizes physiological knowledge to assign performance data to various mask factors at various levels of work. Individual cell entries estimate the percentage performance of a mask wearer, assuming a constant work rate for as long as the work can be performed.

As previously presented[1] the PRT is based on several assumptions.

I. The level of technology is the military full-facepiece, air-purifying M-17 mask.

2. Effects are linear.

3. Wearers are normal, healthy, young adults.

4. Work is performed at a constant rate for as long as possible.

5. Masks and hoods are worn before and after work periods.

6. Task variety increases as performance time increases.

7. Temperate environmental conditions prevail.

The PRT for temperate environments is given in Table 1.The table is organized horizontally by levels of work defined as very light through very heavy (Table II). At the very heavy level, performance time is most likely limited by body biochemistry; for the heavy level, respiratory stress is the most likely limiting factor, for the moderate work rate, thermal burden dominates; and at the light and very light rates of work, long-term factors, such as skin irritation, lack of nourishment, and psychological discomfort, will be the most likely limiting factors.

The PRT is organized vertically by mask factors (e.g., vision) and contributing- mask elements (e.g., acuity and field of view) arranged beneath the mask factors. There are many more possible mask elements that could be included,[1] but efforts were made to reduce the number of elements to a manageable few.

PRT entry values are given as percentages of performance while wearing the M17 mask and hood compared to performance without the mask and hood. All other conditions, including work rate, are considered to be the same regardless of whether the mask is worn.

There are very few experimental results upon which to base the table entry values. As the PRT is presently structured, 75 independent entry values are needed, and this number is much larger than the total number of applicable studies available in the literature. Entry values were thus obtained from the literature, when possible, and from estimates derived from experiences of the authors and others at the U.S. Army Chemical Research Development and Engineering Center at the Aberdeen Proving Grounds. Thus, as indicated in a previous paper,[1] individual entry values may not be entirely correct, but the values that are presently in place, and the PRT method of organization of the data, can be valuable in drawing conclusions regarding mask design and in guiding the conduct of future experimental work.

Overall performance rating is obtained from the individual entry values at any particular work rate as the product of all mask element values or as the product of all mask factor values.[1] The rationale for this approach is based on the fact that all mask factor effects are considered to be independent and that the maximum performance, including one factor, cannot be any higher than that determined by the other factors. Performance decrement is the performance rating subtracted from 100.

Military and industrial respiratory protective masks are used in other than temperate environments, however, and other PRTs were constructed from literature information obtained at three

*Scientific Article No. A6248 Contribution No. 8417 of the Maryland Agricultural Experiment Station (Department of Agricultural Engineering).

other environmental conditions of hot and humid (29°C, 95% RH), hot and dry (49°C, 30% RH), and cold and dry (–32°C, 70% RH).

Entry values for these tables used those for the temperate environment as a starting point. Where differences could clearly be attributed to environmental factors, new estimates were made for performance percentages. Otherwise, table entries duplicated those in the PRT for the temperate environment (Table I).

This paper presents the PRTs for other environmental conditions and the processes that led to their development.

TABLE I. Performance Rating Table for Temperate Environments (20°C)[A]

	Work Rate				
Mask Factor	*Very Light*	*Light*	*Medium*	*Heavy*	*Very Heavy*
Vision	93	95	97	99	99
Field size	96	97	98	100	100
Acuity	97	98	99	99	99
Communications	94	95	98	99	100
Attenuation dist.	99	99	99	99	100
Intelligibility	95	97	99	100	100
Direction	100	99	100	100	100
Respiration	100	98	94	80	81
Resistance	100	99	99	84	84
Dead space	100	99	95	95	96
Thermal Factors	100	95	95	100	100
Moisture removal	100	100	100	100	100
Thermal balance	100	95	95	100	100
Personal Support	93	94	95	95	95
Drinking/eating	93	94	95	95	95
Medical procedures	100	100	100	100	100
Physical Factors	64	69	87	92	97
Physical structure	76	90	98	98	98
Compatibility	85	78	90	95	100
Anthropometry	99	99	99	99	99
Psychological Factors	95	95	98	100	100
Total Performance Rating	49	52	69	69	74
(Total Performance Degradation)	(51)	(48)	(31)	(31)	(26)

[A]Values indicate percent performance of an M-17 mask wearer compared to no-mask performance.

HOT, HUMID CONDITIONS

Thermal Burden

Under hot, humid conditions, thermal factors are an obvious performance degradation factor. James et al.[2] showed that subjects working in the heat (29°C wet-bulb globe temperature [WBGT]) wearing full-facepiece masks averaged 7 or 8 beats/min higher heart rate and 0.2 to 1.3°C higher oral temperature (depending on work rate) than subjects without masks.

Mortagy and Ramsey[3] showed that thermal stress gave a 6% performance decrement when initially placed in a 32°C effective temperature environment. After 1 hr, performance decrement was 15%. This would be expected, because in 1 hr enough time would have passed for the thermal environment to influence body temperature. A steady state was most likely reached in this time.

The National Institute for Occupational Safety and Health (NIOSH) criterion for sedentary workers[4] indicates a hyperbolic relationship between WBGT and performance time in the heat. Up to 240 min may be spent in a 32°C WBGT environment, but only 15 min should be spent at 43°C WBGT. Thus, hot, humid conditions clearly should reduce PRT entry values.

PRT Entry Values

Vision

Vision in an M-17 mask is affected greatly by lens fogging that occurs during hot, humid conditions. Fogging occurs because some of the exhaled moisture and facial skin sweat is trapped inside the mask dead volume and migrates to the lens areas. Under hot, humid conditions, the dew point temperature is quite high and can exceed the ambient temperature. Thus, condensation forms.

Lens fogging is expected to have the greatest effect on performance at the medium work rates. Performance at the highest work rate, lasting 2 min, does not depend as greatly on vision as at the lower work rates. At the lowest two work rates, breathing and sweating will not be heavy enough to result in maximum fogging. A value of about 75% was obtained from unpublished military observations.

Communications

There is no reason to expect communications to be directly affected by these environmental conditions.

Respiration

There is no evidence to support any respiratory differences between hot, humid and temperate conditions. Some exhalation valve popping occurs because of sweat accumulation inside the

mask facepiece, but this was not considered to lead to a significant performance decrement.

Thermal

When determining performance rating for mask thermal factors under hot, humid conditions, total thermal environment for the wearer must be considered. Unlike temperate conditions, where body temperature does not depend strongly on the clothing worn, hot and humid environmental effects can be severe, even at rest, if clothing does not permit

TABLE II. Essential Features of Work Rates Used in the Performance Rating Table[1]

Work Classification	Physical Work Rate (W)	Metabolic Rate (W)	Estimated Performance Time	Example	Description
Very heavy	430	2150	2 min	sprinting	very intense work performed for only a short time
Heavy	240	1190	10 min	running at 4 m/sec	intense work not likely to include much variation of type
Moderate	140	755	50 min	climbing hills, shoveling fast	work at high enough level for a long enough time to significantly increase body temperature
Light	10	202	8 hr	washing clothes, light gymnastics, walking at 0.9 m/sec	significant variation expected in types of tasks performed
Very light	0	105	indefinitely	reading, answering phone, intermittent typing	a wide variety of performed tasks include many involving information transfer

Thermal performance decrement was determined by using the Givoni and Goldman model[5,6] for all work rates despite the more extreme work load range than the model was developed for. Wearers were assumed to have had equilibrated to the environmental conditions before beginning to work at the specified rate.

Thermal characterization of clothing is given by two parameters, clo and im. Clo is a measure of the thermal insulation offered by the clothes. The clo unit was defined in 1941 as the insulation of a normal business suit worn comfortably by sedentary workers in an indoor climate of 21°C.[6] Clo values are measured on a heated copper mannikin. Im is a measure of the impermeability of clothing to water vapor transfer. Im is usually measured on a sweating copper mannikin.

Two clothing ensembles were assumed to be worn: the standard fatigue uniform (clo = 1.4, im = 0.48) and the chemical-biological (CB) overgarment over the fatigue ensemble (clo = 2.11, im = 0.48). The mask and hood (clo = +0.17, im = -0.09) were added as well.

The Givoni and Goldman model was used to calculate the response of deep body temperature to conditions of work, environment, and clothing. It can be used to predict accurately rectal temperature changes during rest, work, and recovery. The sufficient loss of heat model was first used to calculate an equilibrium rectal temperature that would be reached if a long enough time were spent in the specified environment. The rectal temperature time response was then calculated by starting at an initial rectal temperature and aiming toward the equilibrium temperature. Final rectal temperature was taken to be the temperature reached at the end of the assumed performance time for the particular work rate.

Because the model is largely empirical and all relevant details have not been published, a short explanation of the present model usage will be given. Givoni and Goldman[5] gave values for clo and im including a pumping coefficient based upon an effective wind velocity (v_{eff}) composed of actual wind speed and limb movements during exercise. Their values for the standard fatigue uniform were clo = 0.99 $v_{eff}^{-0.25}$ and im = 0.75$_{eff}^{0.25}$ (a typographical error in the published paper listed the latter as im/clo), where the clo and im coefficients (0.99 and 0.75) differ from the measured values (1.4 and 0.48) because of a wind speed different from 1 m/sec when the clo and im values were measured. Goldman[7] stated that measurement wind speed was usually 0.25 or 0.38 m/sec (50 or 75 ft/min). Similar values for the standard fatigue plus overgarment are clo = 1.50

TABLE III. Results of Givoni and Goldman Model for Hot, Humid Environment (29.44°C, 85% RH)

	Final Temperature (°C)			
Work Rate (W)	Std. Fatigue Uniform	Fatigue Uniform with Mask and Hood	Fatigues plus CB Overgarment	CB Overgarment with Mask and Hood
430	37.12	37.26	37.40	37.56
240	37.50	37.69	37.88	37.91
140	38.38	38.68	39.30	39.81
10	37.37	37.53	37.77	37.99
0	37.02	37.16	37.32	37.48

$v_{eff}^{-0.2}$ and $im = 0.51\ v_{eff}^{0.2}$.

When the hood and mask values were added to the model, corrections were made to the overall clo and im values based upon a measured air velocity of 0.25 m/sec and using an effective wind speed exponent of either 0.20 or 0.25, depending on whether the mask and hood were added to the fatigue uniform or the overgarment uniform. In addition, because the mask and hood completely cover the head with an impermeable layer, body surface area available for sweat removal was reduced by 11%. Arguably, removal of that much area for moisture transfer should require that an im correction not be applied to the overall ensemble im value. However, the im correction was applied to account for interference with moisture removal through the neck of the garment. These corrections have no significant effect on the general conclusions that can be drawn from the model results.

Wind speeds that were used were assumed running speeds of 6.7, 4.5, and 2 m/sec for very heavy, heavy, and moderate work rates. The two smallest work rates were assumed to be performed at rest, but slight air movements of 1.5 m/sec were assumed to occur. All wearers were assumed to be heat acclimatized. Results appear in Table III.

For comfort, rectal temperature must be less than 38.2°C.[6] A 25% risk of heat casualties for unacclimatized men exists at a rectal temperature of 39.2°C, a 50% risk at 39.5°C, and a nearly 100% risk at 40°C.[6] If equilibrium temperatures were reached at the highest rates of work, all wearers would become heat casualties. Fortunately, the highest work rates have the shortest performance times, and some final temperatures remain in the comfortable range. Final temperatures for standard fatigues and fatigues with the CB overgarment were similar.

The mask and hood show the greatest effects, as expected, in the light and moderate work ranges, where performance times are long enough and heat generation high enough that final body temperature shows the greatest response.

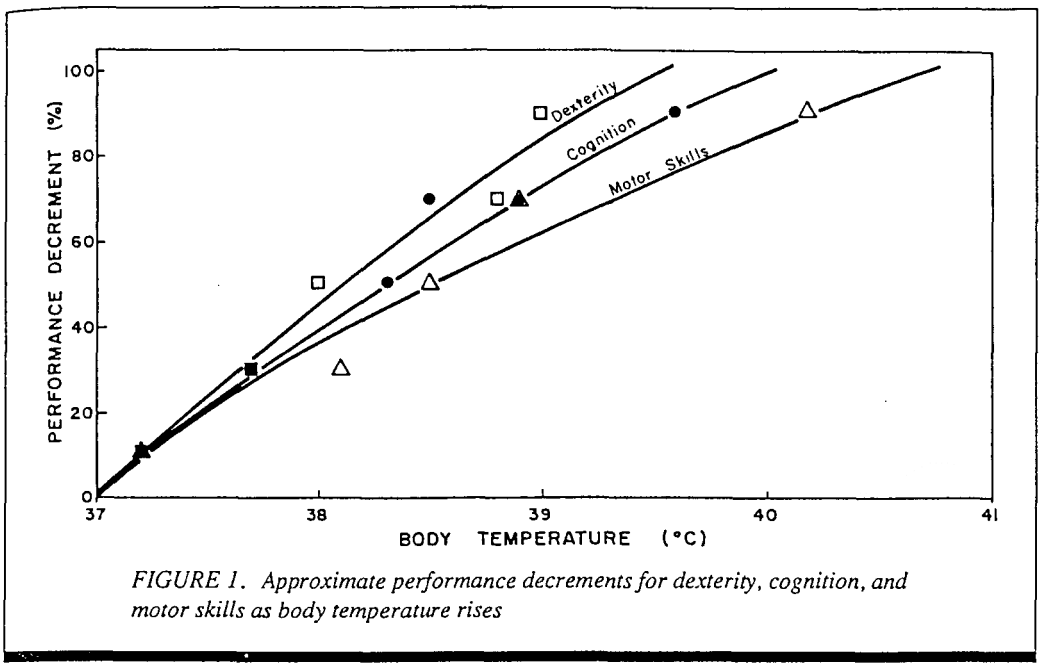

FIGURE 1. Approximate performance decrements for dexterity, cognition, and motor skills as body temperature rises

Performance degradation rates related to deep body temperature for three different performance components: cognition (mental processes), motor skills (gross body movements),and dexterity[8](fine motions) appear in Figure 1. On the basis of the figure, approximate performance decrements were obtained for the various final temperatures listed in Table III. Differences (Table IV) were then used as the basis for the mask thermal factor entries for the PRT for hot, humid environments (Table V). Performance decrements were converted into performance ratings by subtracting decrement values from 100.

Values for thermal performance ratings for the mask and hood appear to be rather high. This is because the majority of thermal performance decrement is the result of the clothing and environment with little contribution by the mask and hood. For the CB overgarment, added values of mask and hood contributions to performance decrement are artificially low because even without the mask and hood, the total performance decrement approaches and cannot exceed 100%.

Personal Support

More time would be required to replenish liquids in the hot, humid environment. Maximum sweating rates would be incurred, and drinking liquid through drinking devices would result in the maximum performance decrement[1] of 25% for the M-17 masks (determined by the required amount of water replenishment and maximum drinking rate), especially for the light and medium rates of work. Liquid replenishment at the highest work rate would not be required for the 2 min of performance.

Physical

There is no reason to expect any performance decrements in addition to those for the temperate environment

Psychological

Mask acceptance, a psychological factor, was shown by Nielsen et al.[9] to be largely determined by environmental factors, but mask temperature and humidity influenced acceptance. Warm, humid breathing air decreased mask acceptance. Their results were obtained with about 80 W external work and quarter-facepiece masks.

TABLE IV. Performance Decrements (%) for Different Clothing and Work Rates for Hot, Humid Conditions (29.44°C, 85% RH)

Work Rate	Std. Fatigue Uniform			Fatigues with Mask and Hood			Difference		
(W)	Dexterity	Cognition	Motor	Dexterity	Cognition	Motor	Dexterity	Cognition	Motor
430	5.7	4.2	3.8	12.6	11.5	9.3	6.9	7.3	5.5
240	23.8	23.1	18.2	32.1	31.4	24.6	8.3	8.3	6.4
140	61.4	58.9	47.3	72.8	68.5	56.0	11.4	9.6	8.7
10	17.5	16.6	13.2	25.1	24.5	19.2	7.6	7.9	6.0
0	1.0	0.0	0.1	7.6	6.3	5.3	6.6	6.3	5.2
Work Rate	CB Overgarment			CB Overgarment with Mask and Hood			Difference		
(W)	Dexterity	Cognition	Motor	Dexterity	Cognition	Motor	Dexterity	Cognition	Motor
430	19.1	18.3	14.4	26.2	25.6	20.1	7.1	7.3	5.7
240	40.6	39.8	31.3	42.0	41.1	32.4	1.4	1.3	1.1
140	94.9	84.8	72.4	100.0	94.1	84.0	5.1	9.3	11.6
10	35.6	35.0	27.4	45.3	44.2	34.9	9.7	9.2	7.5
0	15.5	14.5	11.6	22.7	22.0	17.3	6.5	7.5	5.7

HOT, DRY CONDITIONS

Vision

Because of the higher temperature, dry heat exposure results in greater heat gain, but evaporative heat loss is much greater in the hot, dry condition compared to the hot, humid condition. Because of the low relative humidity that is likely to prevail at such a high temperature, mask fogging will be assumed to be nil despite facial sweating. This will have a major impact on both vision and psychological factors. Vision may suffer somewhat from glare or strong sunlight, but because work could be performed out of direct sunlight, no account was taken of this possibility. Thus, performance ratings were taken to be the same as those for the temperate environment.

TABLE V. Performance Rating Table for Hot, Humid Conditions (29°C, 85% RH)[A]

	Work Rate				
Mask Factor	*Very Light*	*Light*	*Medium*	*Heavy*	*Very Heavy*
Vision	75	75	70	70	75
Field size					
Acuity					
Communications	94	95	98	99	100
Attenuation dist.	99	99	99	99	100
Intelligibility	95	97	99	100	100
Direction	100	99	100	100	100
Respiration	100	98	94	80	81
Resistance	100	99	99	84	84
Dead space	100	99	95	95	96
Thermal Factors	94	92	91	92	93
Moisture removal	98	98	98	98	98
Thermal balance	96	94	93	94	95
Personal Support	75	75	75	90	95
Drinking/eating	75	75	75	90	95
Medical procedures	100	100	100	100	100
Physical Factors	64	69	87	92	97
Physical structure	76	90	98	98	98
Compatibility	85	78	90	95	100
Anthropometry	99	99	99	99	99
Psychological Factors	75	75	75	85	90
Total Performance Rating	24	25	29	36	47
(Total Performance Degradation)	(76)	(75)	(71)	(64)	(53)

[A]Values indicate percent performance of an M-17 mask wearer compared to no-mask performance.

Communications

There is no reason to expect a difference between temperate and hot, dry conditions.

Respiration

No evidence exists to support a difference between temperate and hot, dry conditions.

Thermal

Performance ratings were developed by following the procedure just described for hot, humid conditions. The Givoni and Goldman model[5] was used to estimate final rectal temperatures and, from these, performance decrements were obtained.

Performance rating from thermal factors at the medium work rate was adjusted downward compared to values appearing in Table VII because those values are unduly low with the choices of clothing used. Performance decrement even without the mask and hood became 100% at the medium work rate; the mask and hood could add no more. This process is summarized in Tables VI-V111.

Personal Support

Performance ratings for the drinking/eating element have been taken to be the same as those in the hot, humid environment. There is a somewhat

TABLE VI. Results of Givoni and Goldman Model for Hot, Dry Environment (49°C, 30% RH)

Work Rate (W)	Final Temperature (°C) Std. Fatigue Uniform	Fatigue Uniform with Mask and Hood	Fatigues plus CB Overgarment	CB Overgarment with Mask and Hood
430	38.04	38.23	38.41	38.62
240	38.48	38.70	38.53	38.63
140	39.64	40.36	40.99	41.01
10	38.37	38.67	39.03	39.41
0	37.93	38.12	38.33	38.56

st

ronger possibility of the wearer requiring medical assistance in these extreme conditions compared to temperate conditions, but it is hard to determine values that reflect this higher probability.

Physical

Entry values are the same as temperate condition values. Facial sweat may cause slipping of the mask on the face, but this is difficult to quantify.

Psychological

The lack of lens fogging should assuage development of undue psychological stress. Values were taken to be intermediate between hot, humid values and temperate values.

COLD, DRY CONDITIONS

Vision

A properly fitted M-17 mask will not produce significant fogging in cold, dry conditions. Thus, vision should not degrade performance above that expected for temperate climes.

Communications

Communications performance rating was determined to be identical to temperate conditions, although denser cold air should couple to the voicermitter and stiffen mask material to improve sound transmission.

Respiration

Wearing the mask should somewhat attenuate effects of breathing cold air, but whatever small advantage this effect gives will be placed under thermal factors.

TABLE VII. Performance Decrements (%) for Different Clothing and Work Rates for Hot, Dry Conditions (49°C, 30% RH)

Work Rate (W)	Std. Fatigue Uniform			Fatigues with Mask and Hood			Difference		
	Dexterity	Cognition	Motor	Dexterity	Cognition	Motor	Dexterity	Cognition	Motor
430	47.2	46.1	36.5	55.2	53.4	42.6	8.0	7.3	6.1
240	65.3	62.2	50.3	73.7	69.3	56.7	8.4	7.1	6.4
140	100.0	91.3	80.1	100.0	99.9	94.4	0.0	8.6	14.3
10	60.9	58.5	47.0	72.4	68.2	55.7	11.5	9.7	8.7
0	42.8	41.9	33.1	50.9	49.4	39.3	8.1	7.5	6.2
Work Rate (W)	**CB Overgarment**			**CB Overgarment with Mask and Hood**			**Difference**		
	Dexterity	Cognition	Motor	Dexterity	Cognition	Motor	Dexterity	Cognition	Motor
430	62.4	59.7	48.1	70.5	66.6	54.3	8.1	6.9	6.2
240	67.2	63.9	51.8	71.2	67.1	54.8	4.0	3.2	3.0
140	100.0	100.0	100.0	100.0	100.0	100.0	0.0	0.0	0.0
10	85.6	78.4	65.6	98.5	87.1	75.0	12.9	8.7	9.4
0	59.3	57.0	45.7	68.4	64.9	52.7	9.1	7.9	7.0

Thermal

Although the mask loses heat to both inspired and surrounding air, this heat comes from the face. Close contact between the cold mask and the face could tend to be much more uncomfortable than the face without the mask in still air. In a strong wind, however, the small insulation value of the mask is probably helpful. The mask should have very little thermal effect on the wearer no matter what the work rate because significant amounts of body heat are difficult to accumulate in this climate. Small adjustments in posture or other clothing can easily offset any thermal burden of the mask.

Personal Support

These entry values were taken to be the same as temperate values. It is possible, however, that drinking cannot be accomplished if liquid freezes inside the drinking tube.

Physical

Stiffening of the mask material in cold conditions can exacerbate compatibility and anthropometric elements If the mask facepiece does not bend as well in cold conditions, it will be more difficult to fit to nonnormal facial contours or to conform to mating equipment.

TABLE VIII. Performance Rating Table for Hot, Dry Conditions (49°C, 30% RH)[A]

	Work Rate				
Mask Factor	*Very Light*	*Light*	*Medium*	*Heavy*	*Very Heavy*
Vision	93	95	97	99	99
Field size	96	97	98	100	100
Acuity	97	98	99	99	99
Communications	94	95	98	99	100
Attenuation dist.	99	99	99	99	100
Intelligibility	95	97	99	99	100
Direction	100	99	100	100	100
Respiration	100	98	94	80	81
Resistance	100	99	99	84	84
Dead space	100	99	95	95	96
Thermal Factors	93	90	85	90	93
Moisture removal	98	98	98	98	98
Thermal balance	95	92	87	92	95
Personal Support	75	75	75	90	95
Drinking/eating	75	75	75	90	95
Medical procedures	100	100	100	100	100
Physical Factors	64	69	87	92	97
Physical structure	76	90	98	98	98
Compatibility	85	78	90	95	100
Anthropometry	99	99	99	99	99
Psychological Factors	75	75	75	80	85
Total Performance Rating	29	31	37	47	58
(Total Performance Degradation)	(71)	(69)	(63)	(53)	(42)

[A]Values indicate percent performance of an M-17 mask wearer compared to no-mask performance.

Psychological

onscious awareness of these cold conditions leads to entry of their values under psychological factors rather than thermal factors. Ibis is especially true because adversity tends to heighten awareness of discomfort.

The PRT for the cold environment is given in table IX.

DISCUSSION

In a previous paper,[1] the authors intended to develop a framework leading to better mask design. The ultimate goal of this work must be the replacement of all PRT cellular entries with individual models that

account for various environmental, metabolic, clothing, and situational parameters. Masks are so complex, however, that this goal will not be easily met. Not only do masks modify an individual's physical relationship to his or her surroundings, but masks also interfere with a great deal of the sensory input and life support that the wearer depends on.

An example of how the ultimate goal is to be met is given by the use of the Givoni and Goldman thermal model.[5] This model brings together input information on work rate, environment, and clothing to produce an estimate of final rectal temperature. Next, estimates of performance degradation are obtained corresponding to final rectal temperature. Finally, an estimate of performance rating is obtained from consideration of these performance degradations.

TABLE IX. Performance Rating Table for Cold, Dry Environment (–32°C, 70% RH)[A]

	Work Rate				
Mask Factor	*Very Light*	*Light*	*Medium*	*Heavy*	*Very Heavy*
Vision	93	95	97	99	99
Field size	96	97	98	100	100
Acuity	97	98	99	99	99
Communications	94	95	98	99	100
Attenuation dist.	99	99	99	99	100
Intelligibility	95	97	99	100	100
Direction	100	99	100	100	100
Respiration	100	98	94	80	81
Resistance	100	99	99	84	84
Dead space	100	99	95	95	96
Thermal Factors	100	100	100	100	100
Moisture removal	100	100	100	100	100
Thermal balance	100	100	100	100	100
Personal Support	93	94	95	95	95
Drinking/eating	93	94	95	95	95
Medical procedures	100	100	100	100	100
Physical Factors	57	61	78	82	86
Physical structure	76	90	98	98	98
Compatibility	83	75	88	93	98
Anthropometry	90	90	90	90	90
Psychological Factors	80	80	85	90	100
Total Performance Rating	37	41	56	55	66
(Total Performance Degradation)	(63)	(59)	(44)	(45)	(34)

[A]Values indicate percent performance of an M-17 mask wearer compared to no-mask performance.

Because all details of the Givoni and Goldman model have not been published, it is extremely likely that somewhat incorrect estimates of final rectal temperatures were made. Errors involved in determination of performance decrements are much greater than expected errors in rectal temperatures, thus obscuring errors in the application of the Givoni and Goldman model.

An additional concern involves the variability of mask wearers. The PRT is assumed to apply to the average wearer, but masks must be designed for more sensitive wearers. The degree of variation associated with PRT entries is not known and is extremely difficult to estimate. Even if variance could be assigned to all entries, the most likely combinations of variable factors would still be open to question: a wearer could be more sensitive than normal to respiratory factors or thermal factors, or both. What is the likelihood of both, and should masks be designed for this individual or for less sensitive people?

Even with these questions, the PRT has value as a first step, and better entry values can make the PRT even more valuable. By constructing PRTs for different environments, masks can be seen to have different effects under different conditions. Work performance in hot conditions is degraded so much because of clothing that the mask and hood have little additional effect. Thus, PRT entries can appear extremely promising. If thermal degradation because

of clothing could somehow be solved, then masks and hoods would be seen to degrade performance.

How close most performance ratings are to 100 should be noted in each of these tables. Although total performance ratings may be significantly low, individual mask factor ratings are often in the range of 90-100. This means that performance because of these particular factors is close to the unencumbered performance. The law of diminishing returns indicates that much more design effort will be needed to remove the last few percent of performance degradation. Thus, although the mask gives an overall low performance rating, most of its individual elements are in the area of diminishing returns. For that reason, the mask and hood must be considered from a total systems viewpoint and more total effort should be expected to be expended to make marginal gains.

One other implication of the PRT is that it can show that one mask designed for a wide range of tasks and environments, although feasible, does not optimally satisfy any requirement. The result is that all users are unsatisfied to some extent. Producing masks designed for specific uses would solve this problem. Modular mask elements can reduce the logistical burden of this approach, but to expect mask designers to produce masks that perform optimally for all uses in all environments is unrealistic.

Engineers are taught in school to conceptualize and calculate. Mask design problems, especially those involving performance ratings, have been conceptualized, but not calculated. The result is that anyone who could conceive a new mask concept could become a mask designer, and little distinction between an engineering approach and a trial-and-error approach was made.

The PRT is a first attempt at quantification of mask physiological effects. There are still other steps required before a full calculation procedure is possible. However, it is important for engineers to become knowledgeable in the concepts behind the PRT so that other tables can be constructed for new masks under development. The challenge then will be to produce masks that actually meet performance ratings given in the new tables.

REFERENCES

1. **Johnson, A.T., R.A. Weiss, and C. Grove:** Respirator Performance Rating Table for Mask Design. *Am. Ind. Hyg. Assoc. J.* 53(3):193-202(1992).
2. **James, R., F. Dukes-Dobos, and R. Smith:** Effects of Respirators under Heat/Work Conditions. *Am. Ind. Hyg. Assoc. J.* 45(6):399404(1984).
3. **Mortagy, A.K. and J.D. Ramsey:** Monitoring Performance as a Function of Work/Rest Schedule and Thermal Stress. Am. *Ind. Hyg. Assoc. J.* 34~11):474-480 (1973).
4. **Ramsey, J.D., D. Dayal, and B. Ghahramani:** Heat Stress Limits for the Sedentary Worker. *Am. Ind. Hyg. Assoc. J.* 36(4):259-265 (1975).
5. **Givoni, B. and R.F. Goldman:** Predicting Rectal Temperature Response to Work, Environment, and Clothing. *J. Appl. Physiol.* 32:812-822 (1972).
6. **Johnson, A.T.:** *Biomechanics and Exercise* Physiology. New York: John Wiley& Sons, 1991.
7. **Goldman, R.F.:** "Techniques in Clothing Measurements." October 1990. [Personal Communication]. Comfort-Tech, Framingham, Mass.
8. **Ramirez, T.L., M.E. Rayle, P.A. Crowley, and C.V. Derringer:** The Thermal Effects of the Chemical Defense Ensemble on Human Performance. Human Systems Division USAF, HSD-TR-88-015. Columbus, Ohio: Battelle Memorial Institute, 1988.
9. **Nielsen, R., A.R. Gwosdow, L.G. Berglund, and A.B. DuBois:** The Effect of Temperature and Humidity Levels in a Protective Mask on User Acceptability During Exercise. *Am. Ind. Hyg. Assoc. J.* 48(7):639-645 (1987)

Frontiers Med. Biol. Engng, Vol. 5, No. 4, pp. 265-287 (1993)

ORIGINAL PAPER

How much work is expended for respiration?

ARTHUR T. JOHNSON*
Agricultural Engineering Department and Kinesiology Department (Affiliate), University of Maryland, College Park, MD 20742, USA

Received 10 November 1993; accepted 5 February 1993

Abstract—The rate of work expended to move air in the respiratory system has been determined for five different airflow waveshapes, a non-linear respiratory model and five exercise levels. As expected, the rectangular waveshape was the most efficient. Model conditions were then changed one at a time: (i) starting lung volume was allowed to vary, (ii) exhalation flow limitation was added, (iii) respiration was considered to be metabolic burden determining part of the ventilation requirement and (iv) a respirator mask was added. Although there is no direct work advantage in varying initial lung volume, such volume changes appear to be dictated by the asymmetry of lung recoil pressure about the lung relaxation volume; allowing the work of respiration to become a metabolic burden clearly show why respiratory waveforms change from rest to exercise; and adding a respiratory imposes a severe respiratory burden on the wearer engaging in moderate, heavy and very heavy exercise.

Key words: respiration; work.

1. INTRODUCTION

It has long been assumed that respiration is physiologically adjusted to yield optimum respiration rate, ratio of inhalation time to exhalation time, expiratory reserve volume, dead volume, airways resistance and airflow waveshape. This is especially true during exercise, when the respiratory muscles and skeletal muscles compete for a limited supply of oxygen and other metabolic substrates. Exercise data clearly show change in respiratory parameters consistent with the hypothesis of minimum respiratory work rate.

As part of a larger effort to model the respiratory effects of respiratory masks, the question arose concerning the actual amount of energy that could be saved with modification of the airflow waveshape. Yamashiro and Grodins [1] calculated a 23% lower rate of work if breathing occurred with a rectangular waveshape (constant flow rate) compared with a sinusoidal waveshape. Their calculations were made with a simple respiratory model containing one constant resistance and one constant compliance. Since respiration consumes only 1-2% of the body's oxygen consumption during rest, but up to 10% of the body's oxygen consumption during exercise [2], the effect of airflow waveshape in a model of exercise responses could be significant.

*Scientific Article Number A6418 Contribution Number 8611 of the Maryland Agricultural Experiment Station (Department of Agricultural Engineering)

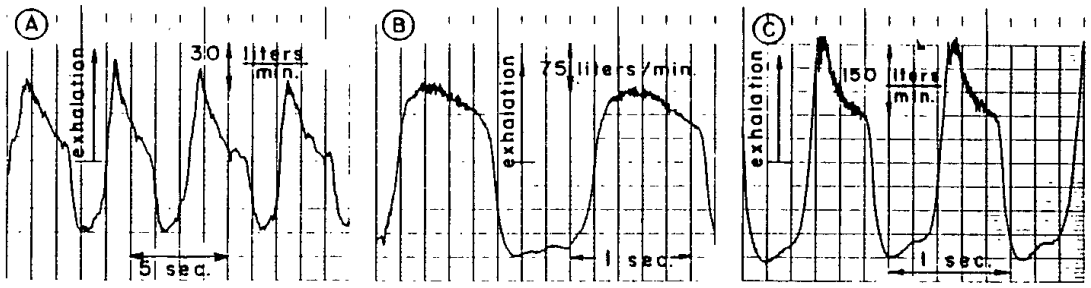

Figure 1. Typical respiratory airflow waveforms during: (a) rest, (b) moderate exercise and (c) extreme exercise.

In Fig. 1, taken from Johnson [2], are found typical respiratory airflow waveshapes for (A) rest, (B) moderate exercise and (C) heavy exercise. During rest, inhalation occurs with a sinusoidal waveshape and exhalation with an exponential waveshape. The sinusoid was found by Yamashiro and Grodins [1] to arise from a mean squared acceleration criterion, and they postulated the sinusoid had an advantage for gas transport efficiency and uniform ventilation of the lungs. Hämäläinen and Viljanen [3] stated that this criterion could result from a penalty associated with inefficient muscular contraction, the possibility of tissue rupture and overstraining, and the difficulty of achieving accurate control at high accelerations. Therefore, the resting inhalation waveform appears to be determined by a measure not related to work rate.

The resting exhalation waveform is exponential, related to the passive nature of exhalation. Energy for this process is derived from the elastic nature of a stretched chest wall and air compressed in the lungs during inhalation. Thus, the resting exhalation waveform, too, is not determined by a minimum work criterion.

Inhalation and exhalation waveforms during moderate exercise appear to be trapezoidal. These contrast somewhat with the rectangular waveform that optimally satisfies a minimum work rate criterion [1, 4]. Ruttiman and Yamamoto [5] gave one explanation for a trapezoidal waveform: they obtained a trapezoidal shape (although with the slope in the wrong direction) when they sought the waveform to minimize work with an airways resistance that increased as lung volume decreased. There is a portion of airways resistance in the lower airways that does exhibit this inverse effect [6].

Hämäläinen and Sipilä [7] gave another possible explanation for the trapezoidal waveform. When they added a term consisting of the squared muscular pressure times the flow rate ($p^2\dot{V}$) to their optimization criterion, to account for decreasing muscular efficiency at higher loads, they obtained a trapezoidal waveform appearing similar to those in Fig. l(B).

Both inhalation and exhalation appear to have become active, and both appear to have waveshapes determined by some measure related to respiratory work rate. Neither waveshape rises immediately to its maximum value, indicating that either (i) the respiratory muscles are of limited strength or (ii) the muscular acceleration is limited to avoid damage or loss of control.

The heavy exercise waveshapes appearing in Fig. 1(C) retain a trapezoidal appearance for inhalation, but return to exponential waveshapes for exhalation. These exhalation waveshapes are usually not elicited until the respiratory system is extremely taxed.

The exponential waveshape is due to the flow rate limitation that accompanies maximal expiratory efforts [8]. If transpulmonary pressure and expiratory flow rate are plotted along lines

of equal lung volume, a point is reached on each of these curves beyond which the flow cannot be increased and may even decrease slightly. This limiting flow rate has been found to be inversely related to lung volume [8]. The exponential waveform during heavy exercise can carry a severe energetic penalty because the flow rates and respiratory muscle pressure are so much higher.

The objectives of this study were to obtain expressions for the rates of work associated with each of these waveforms and to determine the work rate values to be expected during exercise conditions. Using the latter as input information, the need for using different respiratory airflow waveshapes in a larger model of respirator mask wear during exercise can be determined.

2. RESPIRATORY MODEL

It has become fashionable to express respiratory impedances in terms of many elements for the purpose of explaining recent measurement data using forced random noise and forced oscillations [9]. The main interest of the current modelling effort, however, is the respiratory airways, the remainder of the respiratory system and respiratory apparatus affixed to the breathing path. The model to be used, therefore, contains a small number of elements, but nonlinearities appearing in the airways and masks are included (Fig. 2). The model to be used is the modified Rohrer description proposed by Johnson [6], with the addition of compliance and inertance terms:

$$p = K_1\dot{V} + K_2\dot{V}^2 + \frac{K_3\dot{V}}{V} \pm \frac{V - V_r}{C} + I\ddot{V} \qquad (1)$$

where

- p is the respiratory muscle pressure (N/m^2),
- $\dot{V}$ is the respiratory flow rate (m^3/s),
- V is the lung volume (m^3),
- $\ddot{V}$ is the volume acceleration (m^3/s^2),
- V_r is the resting volume of the lung (m^3),
- K_1 is the first Rohrer coefficient for the entire respiratory system ($N\,s/m^5$),
- K_2 is the second Rohrer coefficient ($N\,s^2/m^8$),
- K_3 is the 'third' Rohrer coefficient ($N\,s/m^2$),
- C is the respiratory compliance (m^5/N),
- I is the respiratory inertance ($N\,s^2/m^5$).

There is a dual sign preceding the elastic, or compliant, term. This is because positive inspiratory-elastic work results when $(V - V_r)$ is positive, but positive expiratory work results when $(V - V_r)$ is negative. Values for flow rate are considered to be positive in both inspiratory and expiratory directions, but lung volume can either increase or decrease during the breath.

The value for K_1 includes the traditional first Rohrer coefficient for the airways plus contributions from lung tissue and chest wall. Values for K_2 and K_3 are almost solely due to the airways contribution because there is little nonlinearity or volume dependence in the pressure-flow characteristics of the lung tissue and chest wall [2]. Masks contribute to K_1 and K_2, but not to K_3, and these will be included later.

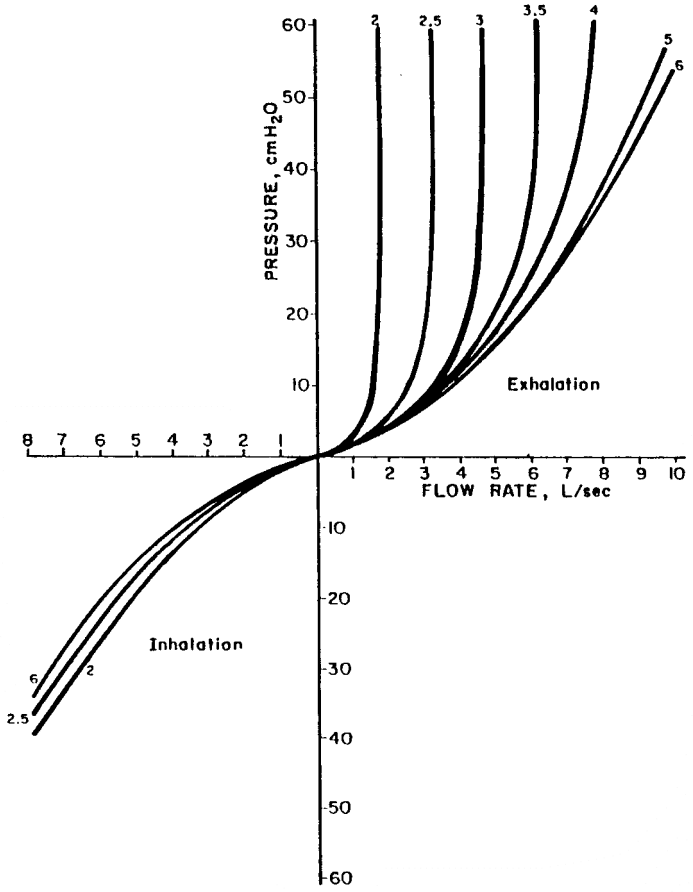

Figure 2. Exhalation and inhalation pressure-flow curves for various lung volumes (in liters) labelled next to their respective curves.

The K_3 term, as given in Johnson [6], appeared as $K_3\dot{V}$ / (V – RV), with the understanding that when lung volume reached residual volume (RV), distensible airways would close and resistance would become infinite [10]. Although there is no reason to dispute that reasoning, removing the RV has not been shown to degrade closeness of fit of curves to data, but removing RV has definite advantages in algebraic and calculus manipulations.

This model form can be applied equally as well to inhalation and exhalation, although there are slight differences in the values of $K_1 - K_3$, C and I for both directions. When flow rate becomes close to and reaches the maximum exhalation flow rate, however, an additional term must be added to equation (1) to account for the apparent increase of airways resistance to infinity:

$$p_e = K_1\dot{V} + K_2\dot{V}^2 + \frac{K_3\dot{V}}{V} \pm \frac{V - V_r}{C} + I\ddot{V} + K_4/(1 - \dot{V}/\dot{V}_L) \qquad (2)$$

where

p_e is the respiratory muscle pressure at airflow limitation (N/m^2),
K_4 is the additional coefficient (N/m^2),
$\dot{V}_L$ is the limiting flow rate (m^3/s).
The last term in this equation appears incorrectly in both [2] and [6].

Average respiratory work rate may be based either on the duration of the waveform (either inspiratory time or expiratory time) or respiratory period. The former choice was taken in order to directly compare the different waveforms.

All lung volumes for the first set of comparisons were assumed to begin at the lung resting volume (equal to functional residual capacity) and were obtained by integrating flow rates. Volume accelerations were obtained by differentiating flow rates.

3. WAVESHAPES

Five different waveshapes were tested: sinusoidal, rectangular, trapezoidal, truncated exponential and hybrid exponential. Diagrams of these appear in Fig. 3. The half-sine wave, trapezoidal and hybrid exponential waveshapes were chosen to mimic waveshapes appearing in Fig. 1. The rectangular waveshape was included as previously identified as the most work rate efficient

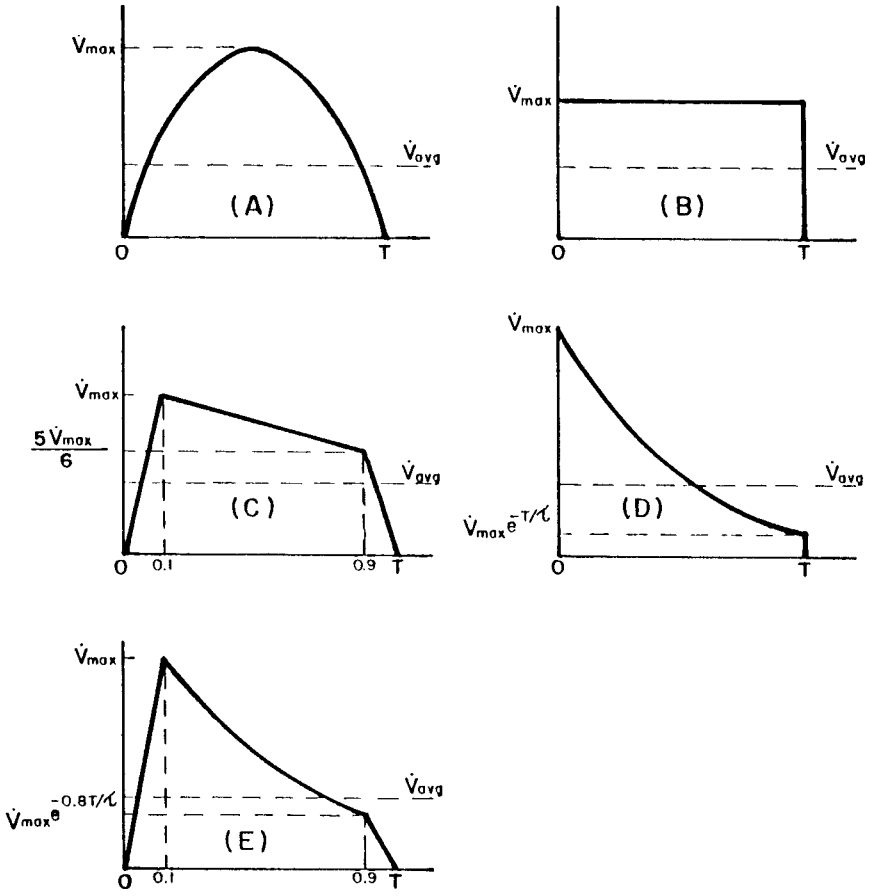

Figure 3. Diagrams of modelled respiratory waveforms: (a) sinusoidal, (b) rectangular, (c) trapezoidal, (d) truncated exponential and (e) hybrid exponential.

shape and the truncated exponential curve was included for personal interest.

Equations for work rates were determined for each waveshape and appear in Table 1. Work rates were determined separately for the five contributing components in equation (1): linear, quadratic, volume dependent, compliant and inertial pressure terms. These are identified in Table 1 as $\dot{W}_R(1)$ through $\dot{W}_R(5)$, and can be recognized by the coefficients that appear in each term. In all cases but one, inertial work rate became identically equal to zero, which, presumably, indicates that work expended to accelerate airflow is counterbalanced by work recovered by decelerating airflow. The only waveform where inertial work was not zero was the truncated exponential shape, where infinite volume acceleration of the idealized waveform made inertial work unable to be calculated for the rising and failing phases. The inertial contribution was not included in total work rate for the truncated exponential waveshape.

Table 1.

Expressions for flow, volume, acceleration and work rate for the five waveshapes

Sinusoidal

$$\dot{V} = \dot{V}_{max} \sin \frac{\pi t}{T} \qquad 0 \leqslant t \leqslant T$$

$$V = V_0 + \frac{\dot{V}_{max} T}{\pi}\left(1 - \cos \frac{\pi t}{T}\right)$$

$$\ddot{V} = \pm \frac{\dot{V}_{max} T}{\pi} \cos \frac{\pi t}{T}$$

$$V_T = 2\dot{V}_{max} T/\pi$$

$$\dot{V}_{avg} = 2\dot{V}_{max}/\varepsilon\pi$$

$$\dot{W}_R(1) = K_1 \dot{V}_{max}^2/2$$

$$\dot{W}_R(2) = 4K_2 \dot{V}_{max}^3/3\pi$$

$$\dot{W}_R(3) = K_3 \dot{V}_{max} \pi \left(a - \sqrt{a^2 - 1}\right)$$

$$a = \frac{V_0 \pi}{\dot{V}_{max} T} \pm 1$$

$$\dot{W}_R(4) = 2\dot{V}_{max}^2 T/\pi^2 C \pm V_T(V_0 - V_t)/TC$$

$$\dot{W}_R(5) = 0$$

Rectangular

$$\dot{V} = \dot{V}_{max} \qquad 0 \leqslant t \leqslant T$$

$$V = V_0 + \dot{V}_{max} t$$

$$\ddot{V} = 0 \qquad 0 < t < T$$

$$V_T = \dot{V}_{max} T$$

$$\dot{V}_{avg} = \dot{V}_{max}/\varepsilon$$

$$\dot{W}_R(1) = K_1 \dot{V}_{max}^2$$

Table 1.
(Continued)

$$\dot{W}_R(2) = K_2 \dot{V}_{max}^3$$

$$\dot{W}_R(3) = \pm \frac{K_3 \dot{V}_{max}}{T} \log \left(1 \pm \frac{\dot{V}_{max} T}{V_0} \right)$$

$$\dot{W}_R(4) = \frac{\dot{V}_{max} T}{2C} \pm V_T(V_0 - V_r)/TC$$

$$\dot{W}_R(5) = 0$$

Trapezoidal

$$\dot{V} = 10\dot{V}_{max} t/T \qquad 0 \leqslant t \leqslant 0.1T$$

$$\dot{V} = \frac{\dot{V}_{max}}{48} (49 - 10t/T) \qquad 0.1T \leqslant t \leqslant 0.9T$$

$$\dot{V} = \frac{25\dot{V}_{max}}{3} (1 - t/T) \qquad 0.9T \leqslant t \leqslant T$$

$$V = V_0 + 5\dot{V}_{max} t^2/T \qquad 0 \leqslant t \leqslant 0.1T$$

$$V = V_0 + \frac{\dot{V}_{max}}{48} (-2.45T + 49t - 5t^2/T) \qquad 0.1T \leqslant t \leqslant 0.9T$$

$$V = V_0 + \frac{25\dot{V}_{max}}{3} (-0.401T + t - t^2/2T) \qquad 0.9T \leqslant t \leqslant T$$

$$\ddot{V} = 10\dot{V}_{max}/T \qquad 0 \leqslant t \leqslant 0.1T$$

$$\ddot{V} = -\dot{V}_{max}/4.8T \qquad 0.1T \leqslant t \leqslant 0.9T$$

$$\ddot{V} = -25\dot{V}_{max}/3T \qquad 0.9T \leqslant t \leqslant T$$

$$V_T = 0.825\dot{V}_{max} T$$

$$\dot{V}_{avg} = 0.825\dot{V}_{max}/\epsilon$$

$$\dot{W}_R(1) = 0.730556 K_1 \dot{V}_{max}^2$$

$$\dot{W}_R(2) = 0.8129416 K_2 \dot{V}_{max}^3$$

$$\dot{W}_R(3,1) = 2 - 2S \tan^{-1}(1/S) \qquad S^2 > 0$$

$$\dot{W}_R(3,1) = -2 + S \log \left(\frac{S+1}{S-1} \right) \qquad S^2 < 0$$

where

$$S = \sqrt{\frac{20V_0}{\dot{V}_{max} T}}$$

$$\dot{W}_R(3,2) = \frac{2}{q} \left[\pm 0.4166667 \frac{V_0}{\dot{V}_{max} T} + 1.020833 \right] \times \left[\tan^{-1} \left(\frac{1.0104167}{q} \right) - \tan^{-1} \left(\frac{0.9270833}{q} \right) \right] \mp 0.3333333 \qquad q^2 > 0$$

$$\dot{W}_R(3,2) = \left(\pm 0.4166667 \frac{V_0}{\dot{V}_{max} T} + 1.020833 \right) \frac{L_2}{q} \mp 0.3333333 \qquad q^2 < 0$$

Table 1.
(Continued)

$$q = \sqrt{\mp \frac{0.4166667 V_0}{\dot{V}_{\max} T} - 1.020833}$$

$$L_2 = \pm \log \left[\frac{(q+1)}{(q-1)} \frac{(q-0.8333333)}{(q+0.83333333)} \right]$$

$$\dot{W}_R(3,3) = \frac{2}{p} \left[-16.66667 \frac{V_0}{\dot{V}_{\max} T} \mp 13.75 \right] \tan^{-1} \left(\frac{0.8333333}{p} \right) \mp 1.666667 \qquad p^2 > 0$$

$$\dot{W}_R(3,3) = \left(\pm 16.666667 \frac{V_0}{\dot{V}_{\max} T} + 13.75 \right) \frac{L_3}{p} \mp 1.66667 \qquad p^2 < 0$$

$$p = \sqrt{\mp \frac{16.66667 V_0}{\dot{V}_{\max} T} - 13.75}$$

$$L_3 = \pm \log \left(\frac{p + 0.8333333}{p - 0.8333333} \right)$$

$$\dot{W}_R(3) = \frac{K_3 \dot{V}_{\max}}{T} \left[\dot{W}_R(3,1) + \dot{W}_R(3,2) + \dot{W}_R(3,3) \right]$$

$$\dot{W}_R(4) = 0.3403343 \frac{\dot{V}_{\max}^2 T}{C} \pm V_T (V_0 - V_r)/TC$$

$$\dot{W}_R(5) = 0$$

Truncated exponential

$$\dot{V} = \dot{V}_{\max} e^{-t/\tau} \qquad 0 \leqslant t \leqslant T$$

$$V = V_0 \pm \dot{V}_{\max} \tau (1 - e^{-t/\tau})$$

$$\ddot{V} = \mp \frac{\dot{V}_{\max}}{\tau} e^{-t/\tau}$$

$$V_T = \dot{V}_{\max} \tau (1 - e^{-T/\tau})$$

$$\dot{V}_{avg} = \dot{V}_{\max} \tau (1 - e^{-T/\tau})/\epsilon T$$

$$\dot{W}_R(1) = \frac{K_1 \dot{V}_{\max}^2 \tau}{2T} (1 - e^{-2T/\tau})$$

$$\dot{W}_R(2) = \frac{K_2 \dot{V}_{\max} \tau}{3T} (1 - e^{3T/\tau})$$

$$\dot{W}_R(3) = \frac{K_3 \dot{V}_{\max}}{T} \left[\pm e^{-T/\tau} \log g_T + \frac{V_0}{\dot{V}_{\max} \tau} (g_T \log g_T - g_T + 1) \right]$$

$$g_T = 1 \pm \frac{\dot{V}_{\max} \tau}{V_0} (-e^{-T/\tau})$$

$$\dot{W}_R(4) = \frac{\dot{V}_{\max}^2 \tau^2}{2CT} (1 - e^{-T/\tau})^2 \pm V_T (V_0 - V_r)/TC$$

$$\dot{W}_R(5) = -\frac{I \dot{V}_{\max}^2}{2} (1 - e^{-2T/\tau})$$

Table 1.
(Continued)

Hybrid exponential

$$\dot{V} = 10\dot{V}_{max}t/T \qquad 0 \leqslant t \leqslant 0.1T$$

$$\dot{V} = \dot{V}_{max}e^{0.1T/\tau}e^{-t/\tau} \qquad 0.1T \leqslant t \leqslant 0.9T$$

$$\dot{V} = 10\dot{V}_{max}e^{-0.8T/\tau}(1 - t/T) \qquad 0.9T \leqslant t \leqslant T$$

$$V = V_0 + 5\dot{V}_{max}t^2/T \qquad 0 \leqslant t \leqslant 0.1T$$

$$V = V_0 + 0.05T\dot{V}_{max} + \tau\dot{V}_{max}e^{0.1T/\tau}(e^{-0.1T/\tau} - e^{-t/\tau}) \qquad 0.1T \leqslant t \leqslant 0.9T$$

$$V = V_0 + \dot{V}_{max}\left[0.05T + \tau(1 - e^{-0.8T/\tau}) + 10e^{-0.8T/\tau}(t - t^2/2T - 0.495T)\right] \qquad 0.9T \leqslant t \leqslant T$$

$$\ddot{V} = \pm 10\dot{V}_{max}/T \qquad 0 \leqslant t \leqslant 0.1T$$

$$\ddot{V} = \mp\frac{\dot{V}_{max}}{\tau}e^{0.1T/\tau}e^{-t/\tau} \qquad 0.1T \leqslant t \leqslant 0.9T$$

$$\ddot{V} = \mp\frac{10\dot{V}_{max}}{T}e^{-0.8T/\tau} \qquad 0.9T \leqslant t \leqslant T$$

$$V_T = \dot{V}_{max}\left[\tau(1 - e^{-0.8T/\tau}) + 0.05T(1 + e^{-0.8T/\tau})\right]$$

$$\dot{V}_{avg} = \dot{V}_{max}\left[\tau(1 - e^{-0.8T/\tau}) + 0.05T(1 + e^{-0.8T/\tau})\right]/\varepsilon T$$

$$\dot{W}_R(1) = \frac{K_1\dot{V}_{max}^2}{2T}\left[T(1 + e^{-1.6T/\tau})/15 + \tau(1 - e^{-1.6T/\tau})\right]$$

$$\dot{W}_R(2) = \frac{K_2\dot{V}_{max}^3}{T}\left[T(1 + e^{-2.4T/\tau})/40 + \tau(1 - e^{-2.4T/\tau})/3\right]$$

$$\dot{W}_R(3,1) = 2 - 2S\tan^{-1}(1/S) \qquad S^2 > 0$$

$$\dot{W}_R(3,1) = -2 + S\log\left(\frac{S+1}{S-1}\right) \qquad S^2 < 0$$

$$S = \frac{\sqrt{20V_0}}{\dot{V}_{max}T}$$

$$\dot{W}_R(3,2) = \mp(1 - e^{-0.8T/\tau}) - \frac{L_5T}{\tau}\left(\frac{V_0}{\dot{V}_{max}T} \pm 0.05 \pm \frac{\tau}{T}\right)$$

$$L_5 = \log\left[\frac{V_0/T\dot{V}_{max} \pm 0.05}{V_0/T\dot{V}_{max} \pm 0.05 \pm \frac{\tau}{T}(1 - e^{0.8T/\tau})}\right]$$

$$\dot{W}_R(3,3) = \frac{2}{r}\left(\mp 100e^{-1.6T/\tau} - 20ae^{-0.8T/\tau}\right)\tan^{-1}\left(\frac{e^{-0.8T/\tau}}{r}\right) \mp 2e^{-0.8T/\tau} \qquad r^2 > 0$$

$$\dot{W}_R(3,3) = \left(100e^{-1.6T/\tau} \pm 20ae^{-0.8T/\tau}\right)\frac{L_6}{r} \mp 2e^{-0.8T/\tau} \qquad r^2 < 0$$

$$r = \sqrt{\mp 20ae^{-0.8T/\tau} - 100e^{-1.6T/\tau}}$$

$$a = \frac{V_0}{\dot{V}_{max}T} \pm 0.05 \pm \frac{\tau}{T}(1 - e^{-0.8T/\tau}) \mp 4.95e^{-0.8T/\tau}$$

$$L_6 = \pm\log\left[\frac{r + e^{-0.8T/\tau}}{r - e^{-0.8T/\tau}}\right]$$

Table 1.
(Continued)

$$\dot{W}_R(3) = \frac{K_3 \dot{V}_{max}}{T}\left[\dot{W}_R(3,1) + \dot{W}_R(3,2) + \dot{W}_R(3,3)\right]$$

$$\dot{W}_R(4) = \frac{\dot{V}_{max}^2}{CT}\left\{\frac{T^2}{800} + \tau(0.05T + \tau)(1 - e^{-0.8T/\tau}) + \frac{\tau^2}{2}(1 - e^{-1.6T/\tau}) + e^{-0.8T/\tau} \times \left[T^2(0.0025 + 0.00125e^{-0.8T/\tau}) + 0.05\tau T(1 - e^{-0.8T/\tau})\right]\right\} \pm V_T(V_0 - V_r)/TC$$

$$\dot{W}_R(5) = 0$$

Trapezoidal and hybrid exponential flows, volumes, and accelerations are defined separately for the three time periods: $0 \leq t \leq 0.1T$, $0.1T \leq t \leq 0.9T$ and $0.9T \leq t \leq T$.

Tidal volume (V_T) is the volume of air that accumulates during each breath, and thus is the total volume of air for each waveform.

Average flow rate over the entire respiratory period was also calculated from:

$$\dot{V}_{avg} = V_T/\varepsilon T \qquad (3)$$

where

$\dot{V}_{avg}$ is the average flow rate (m^3/s),
V_T is the tidal volume (m^3),
T is the duration of waveform (s),
E is the dimensionless conversion between duration of breathing phase and respiratory period ($1 + t_e/t_i$ for $T = t_i$; $1 + t_i/t_e$ for $T = t_e$),
t_i is the inhalation time (s),
t_e is the exhalation time (s).

Average flow rate acknowledges the fact that lung filling with fresh air occurs only during inhalation. Average flow rates remained the same for each waveshape, but varied with work rates. Maximum flow rate were calculated for each waveshape.

Values used in this simulation were:

K_1(aw) = 10^5 N s/m^5
K_2(aw) = 10^7 N s^2/m^8
K_3(aw) = 125 N s/m^2
K_1(lt) = 4 x 104 N s/m^5
K_1(cw) = 2 x 10^5 N s/m^5
K_2(lt) = K_3(lt) = K_2(cw) = K_3(cw) = 0
C(aw) = 0 m^5/N
C(lt) = C(cw) = 2 x 10^{-6} m^5/N
I = 2600 N s^2/m^5

where

(aw) = airway
(lt) = lung tissue
(cw) = chest wall

and

$$K_1 = K_1(\text{aw}) + K_1(\text{lt}) + K_1(\text{cw}) \tag{4}$$

$$C = C(\text{lt})C(\text{cw}) / [C(\text{lt}) + C(\text{cw})] \tag{5}$$

The respiratory time constant was calculated from

$$\tau = RC = [K_1 + K_2 \dot{V}_{\text{avg}} \varepsilon + K_3 / (V_0 \pm V_T/2)]C \tag{6}$$

where

τ is the time constant (s),
R is the respiratory resistance (N s/m^5),
V_0 is the initial lung volume (m^3),

which uses average flow rate over the waveshape and average lung volume during the waveshape. Initial lung volume was assumed to be FRC = 0.0025 m^3. Where a dual sign appears, the top sign corresponds to inhalation and the bottom sign to exhalation. Average flows, inhalation times and exhalation times are given in Table 2 for exercise conditions of rest, light, moderate, heavy and very heavy.

Table 2.
Parameter values used for the comparison of respiratory work rates between different waveshapes

	Minute volume (m^3/s)	Inhalation time (s)	Exhalation time (s)
Rest	1.333333×10^{-4}	1.5	3
Light	2.5×10^{-4}	1.25	2
Moderate	8.333333×10^{-4}	1	1.1
Heavy	1.333333×10^{-3}	0.7	0.75
Very heavy	1.833333×10^{-3}	0.5	0.5

4. COMPARING WORK RATES

Results from this comparison appear in Tables 3 and 4. As expected, the rectangular waveform gave the lowest work rates for all four exercise levels. This is the result of the lowest maximum flow rate of any waveshape. Expressions appearing in Table 1 clearly show the penalty paid for higher maximum flow rates, with $\dot{V}^2_{\text{max}}$ and $\dot{V}^3_{\text{max}}$ terms appearing often.

Using the rectangular waveform as a base, the sinusoidal inspiratory waveform costs from 9% more at light exercise to 16% more at very heavy exercise. There is not a great penalty paid for breathing with a trapezoidal waveshape: the trapezoid costs 3% more at light exercise, increasing to 7% more at very heavy exercise.

Table 3.
Work rate contributions for different components for each waveshape at light work during inhalation at fixed initial lung volume

	Sinusoidal	Rectangular	Trapezoidal	Truncated exponential	Hybrid exponential
$\dot{V}_{max}$	10.2×10^{-3}	6.50×10^{-4}	7.88×10^{-4}	21.7×10^{-4}	19.0×10^{-4}
$\dot{W}_R(1)$	0.177	0.144	0.154	0.250	0.232
$\dot{W}_R(2)$	4.52×10^{-3}	2.75×10^{-3}	3.96×10^{-3}	10.7×10^{-3}	8.88×10^{-3}
$\dot{W}_R(3)$	2.25×10^{-2}	1.83×10^{-2}	1.97×10^{-2}	3.32×10^{-2}	3.05×10^{-2}
$\dot{W}_R(4)$	0.264	0.264	0.264	0.264	0.264
$\dot{W}_R(5)$	0	0	0	-4.91×10^{-3}	0
Total	0.468	0.429	0.442	0.558	0.535

Flow rates in m^3/s, work rates as N m/s. Truncated exponential total work rate excludes $\dot{W}_R(5)$. Initial lung volume is FRC = 0.0025 m^3.

Table 4.
Total rates of work (N m/s) at five levels of exercise for the five waveshapes during inhalation and exhalation at fixed initial lung volume

	Sinusoidal	Rectangular	Trapezoidal	Truncated exponential	Hybrid exponential
Inhalation					
rest	0.197	0.182	0.187	0.248	0.235
light	0.468	0.429	0.442	0.558	0.535
moderate	3.05	2.74	2.85	3.41	3.33
heavy	6.56	5.76	6.06	6.63	6.65
very heavy	10.4	8.93	9.53	9.75	9.98
Exhalation					
rest	0.0797	0.0760	0.0778	0.121	0.108
light	0.248	0.232	0.237	0.335	0.311
moderate	2.78	2.51	2.60	3.05	2.99
heavy	6.31	5.56	5.83	6.21	6.26
very heavy	11.3	9.64	10.2	10.2	10.5

Initial lung volume is FRC = 0.0025 m^3.

The trends for the inspiratory exponential waveshape costs are opposite from the others. The truncated exponential costs 30% more at light exercise, decreasing to 9% more at very heavy exercise. The inspiratory hybrid exponential costs 29% more at light exercise, decreasing to 12% more at very heavy exercise. These trends are the result of shortening the inhalation time as exercise proceeds. Calculated time constant remains at about 0.39 s and, with shorter waveform duration, the exponential waveshapes more closely approach the trapezoidal waveshape as exercise intensity increases. Because of this, maximum flow rates relative to the trapezoidal and sinusoidal waveshapes decrease with exercise for the exponential waveshapes.

Exhalation work rates were generally lower than inhalation work rates as a result of exhalation times longer than inhalation times. As exhalation time shortens, exhalation work rates overtake inhalation work rates. This is because the $\dot{W}_R(3)$ component depends inversely on lung volume, which is higher during inspiration than expiration as long as initial lung volume is fixed at FRC.

All elastic work terms were calculated to be identical for all waveshapes. This is a consequence of setting all average flow rates equal, since all elastic work rate terms became:

$$\dot{W}_R(4) = \frac{\dot{V}_{avg}^2 \varepsilon^2 T}{2C} \tag{7}$$

Johnson [2] gives the value of physical work for circulation and respiration for rest as 2 N m/s and for light activity as 6 N m/s. He also estimates resting cardiac power output at about 1.8 N m/s. Values appearing in Table 4 are thus very reasonable in magnitude.

Efficiency of the respiratory muscles has been estimated at 7–11% [2]. Total physiological work demands on the body are thus about 10 times the amounts appearing in Table 3. The energy cost of very light work has been estimated at 183 N m/s [2]. The sinusoidal waveshape, assuming passive exhalation, gives an energy cost of about 4.68 N m/s, or 3% of the body's energy expenditure. The energy cost of heavy work is about 707 N m/s. The values from Table 3, assuming active inhalation and exhalation, both using trapezoidal waveform, give 118.9 N m/s energy cost of respiration, or about 17% of the total. This number is expected to be about half that percentage. One difference between these results and expectations is that, for all conditions except resting, lung volume does not begin at FRC. Since one of the largest contributors to the total work rate, in most cases, is elastic work ($\dot{W}(4)$), a change in beginning position of the lung can have a significant effect on total energy cost. For instance, elastic work for an expiratory trapezoidal waveform beginning at FRC during heavy work is 5.83 N m/s, whereas for the same exhalation waveform beginning at FRC + V_T elastic work is 0.442 N m/s (Table 5). A trapezoidal inhalation beginning at FRC followed by a trapezoidal exhalation beginning at FRC + V_T expends about 65 N m/s physiological work, or 9% of the total cost of heavy exercise.

Table 5.
Work rate contributions (N m/s) for different components for the trapezoidal waveshape for two different initial lung volumes during heavy work

	Initial volume			
	FRC (exhalation)	FRC + V_T (exhalation)	FRC (inhalation)	FRC + V_T (inhalation)
$\dot{W}_R(1)$	2.42	2.42	2.78	2.78
$\dot{W}_R(2)$	0.248	0.248	0.305	0.305
$\dot{W}_R(3)$	0.661	0.261	0.305	0.192
$\dot{W}_R(4)$	2.49	−2.49	2.67	8.01
$\dot{W}_R(5)$	0	0	0	0
Total	5.83	0.442	6.06	11.3

$\dot{V}_{avg} = 3.35 \times 10^{-3}$ m^3/s for inhalation; $\dot{V}_{avg} = 3.12 \times 10^{-3}$ m^3/s for exhalation; $t_i = 0.7$ s; $t_e = 0.75$ s.

5. VARIABLE LUNG VOLUME

Expiratory reserve volume (ERV), or the difference between the residual volume (RV) and the minimum lung volume reached during a breath, can change as exercise and the depth of breathing changes. To account for the effect of a change in the initial lung volume on total work rate it is necessary to attend to the two work components including volume in their calculations. The only necessary correction to $\dot{W}_R(3)$ is to insert the correct initial volume where indicated. The correction to $\dot{W}_R(4)$, the elastic work, is an addition of the form:

$$\frac{1}{TC}\int_0^T (V_0 - V_r)\dot{V}dt = \frac{(V_0 - V_r)V_T}{TC} \tag{8}$$

This term should be subtracted from exhalation work rate and added to inhalation work rate because lung stretching above the relaxation volume aids exhalation but inhibits inhalation.

In this modelling exercise, V_T, V_r and C are held constant for any given exercise condition. Since terms of the form of equation (8) are of the same magnitude but of opposite sign for inhalation and exhalation, there is no net work rate advantage to changing lung volume when considered over the whole breathing cycle as long as exhalation is active and muscular efficiencies are the same in both directions.

Yamashiro and Grodins [11] and Yamashiro *et al.* [12] presented methods to calculate optimal ERV to minimize respiratory work rate when considered over the entire breathing cycle. However, they did not consider that elastic work is stored work, i.e. recovered during the breathing cycle. Thus, their method is in error on this point.

An alternate explanation may be found for the apparent change in ERV during exercise by considering the nonlinear pressure-volume (p-V) characteristic of the lung (Fig. 4). The relationship between elastic pressure and lung volume, as most p-V characteristics of biological organs and tissues, becomes flatter as volume extremes are reached. Compliance is taken to be the ratio of volume change to pressure change, and so decreases at the extreme ends.

Johnson [13] used these data as an example for his curve-fitting program and found that:

$$\frac{\text{VC}}{V - \text{RV}} = 1.00 + \exp(b - cp) \tag{9}$$

where

p is the pressure (N/m^2),
VC is the vital capacity (m^3),
RV is the residual volume (m^3),
b and c are coefficients (dimensionless and m^2/N).

He found the value of b to be about 1.00 and c to be about 1.80 x 10^{-3} m^2/N.

One reason for the shifting of lung position as tidal volume increases may be the asymmetrical nature of the p–V curve around the relaxation volume. Thus, if lung position did not shift, a higher muscle pressure would be required in the exhalation direction compared to inhalation. There may be an efficiency disadvantage if such an imbalance existed.

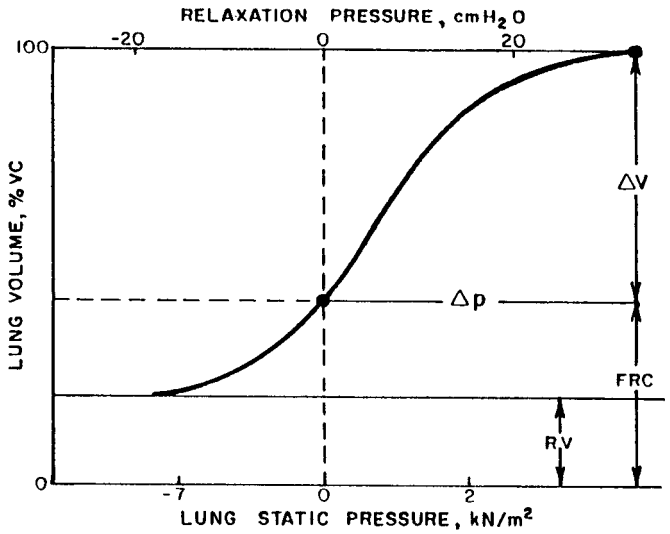

Figure 4. Lung *p-V* curve, excluding hysteresis that often appears. Compliance is the slope of the curve, becoming smaller at extremes of lung volume. Note the asymmetry of the curve around FRC (or relaxation volume), taken to be the lung mid position during breathing at rest.

Equation (9) can be solved for pressure, and maximum inspiratory and expiratory pressures can be made equal. This gives

$$V_{oe} = VC \times \frac{\left(\frac{VC}{V_{oi} - RV} - 1.00\right) + 1.00}{e^{2b}} + RV \qquad (10)$$

where

V_{oe} is the minimum expiratory lung volume (m^3) and
V_{oi} is the maximum inspiratory lung volume (m^3).

Also,

$$V_T = V_{oi} - V_{oe} \qquad (11)$$

and

$$V_m = V_{oe} + V_T/2 \qquad (12)$$

where V_m is the lung midposition (m^3).

Thus, the relationship between V_{oi}, V_{oe}, V_m and V_T may be determined, and is plotted in Fig. 5. Also plotted on the graph are data from Asmussen and Christensen that appeared in Yamashiro and Grodins [11]. These data have been adjusted so that the lung midposition is the same as V_m (= 2.66 x $10^{-3}m^3$) from equation (12) at a tidal volume of 1.69 x $10^{-3}m^3$. Except for the data at low tidal volume, taken under resting conditions, the same shape curve seems to be indicated by both data and calculations. Thus the equal pressure hypothesis appears to be a reasonable explanation for the shift in lung position as breathing deepens.

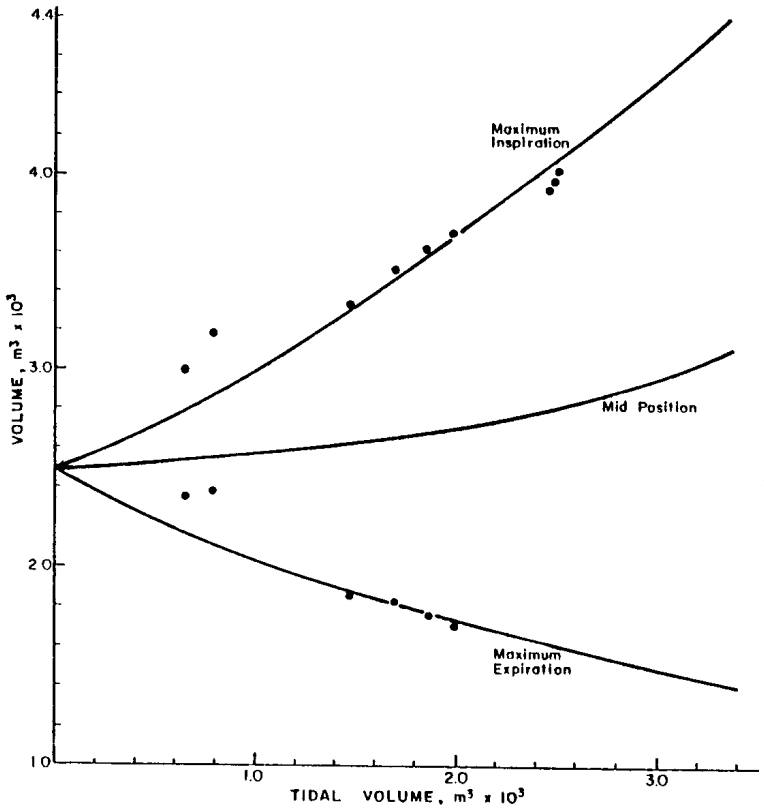

Figure 5. Inspiratory and expiratory initial lung volumes and lung mid position calculated from an assumption of equal inspiratory and expiratory elastic pressures. Data points are from Asmussen and Cbristensen appearing in Yamashiro and Grodins (1973), and adjusted so that lung mid position is 2.66 x 10^{-3} m^3 at a tidal volume of 1.69 x 10^{-3} m^3.

Table 6.
Work rate contributions (N m/s) for different components for the trapezoidal waveshape for heavy work during inhalation and exhalation at fixed and variable initial lung volumes

	Inhalation		Exhalation	
Initial lung volume	FRC (2.5×10^{-3} m^3)	variable (1.74×10^{-3} m^3)	FRC (2.5×10^{-3} m^3)	variable (3.67×10^{-3} m^3)
Component				
$\dot{W}_R(1)$	2.78	2.78	2.43	2.43
$\dot{W}_R(2)$	0.305	0.305	0.248	0.248
$\dot{W}_R(3)$	0.305	0.398	0.661	0.339
$\dot{W}_R(4)$	2.67	0.575	2.49	−0.537
$\dot{W}_R(5)$	0	0	0	0
Total	6.06	4.06	5.83	2.48

$\dot{V}_{max} = 3.35 \times 10^{-3}$ m^3/s (inhalation); $\dot{V}_{max} = 3.12 \times 10^{-3}$ m^3/s (exhalation); $t_i = 0.7$ s; $t_e = 0.75$ s.

There is no first order energy cost consequence for this lung position shift. When corrected for different inhalation and exhalation times, total elastic work (instead of work rate) becomes zero for conditions appearing in Tables 5 and 6. The only component asymmetrically affected by a change in initial lung volume is the $\dot{W}_R$ (3), but its contribution is relatively minor.

6. MAXIMUM EXPIRATORY FLOW

Due to a partial collapse of distensible air passages when subjected to high external pressures and high internal flow rates, respiratory flow rates become limited during maximal exertion. Limited expiratory flows have been found to be related to respiratory distress and voluntary termination of exercise while wearing a respirator mask [14] but not while exercising without a mask [15]. When the flow limitation is reached, incremental respiratory resistance approaches infinity. Sometimes, flow rate is even seen to decrease when limited, and flows may become unstable [16].

Limited exhalation flow rate has been found [6, 8] to be dependent on lung volume

$$\dot{V}_L = \frac{1}{\tau}(V - \mathrm{RV}) \tag{13}$$

where

$\dot{V}_L$ is the limiting flow rate (m^3/s),
τ is the respiratory time constant (s),
V is the lung volume (m^3),
RV is the lung residual volume (m^3).

To obtain this result, an assumption of linearity was made for the typical flow-volume loop obtained during pulmonary function testing [8]. Actually, the flow volume loop is not entirely linear, but over the normal range of lung volumes encountered during exercise, a linearity assumption is quite reasonable.

In temporal terms, the exponential portion of the hybrid exponential waveform describes limited flow rate well:

$$\dot{V}_L = \dot{V}_{max} e^{-(t-0.17T)/\tau} \tag{14}$$

The $(t - 0.1T)$ term translates time for the exponential curve.

Equating limiting flow rate in equation (14) with that in equation (13), and substituting the expression for volume found in Table 1 for the hybrid exponential curve during exhalation gives:

$$\frac{1}{\tau}\left[V_0 - 0.05T\dot{V}_{max} - \tau\dot{V}_{max} + \tau\dot{V}_{max} e^{-(t-0.1T)/\tau} - \mathrm{RV}\right] = \dot{V}_{max} e^{-(t-0.1T)/\tau} \tag{15}$$

Thus

$$V_0 = 0.05T\dot{V}_{max} + \dot{V}_{max}\tau + \mathrm{RV} \tag{16}$$

meaning that initial lung volume must vary with maximum flow rate to give the exponential decay of flow seen in Fig. 1(C). Initial volume calculated from equation (16) has been found to differ by only 1 – 2% from initial volume calculated by means of equations (10) and (11).

A term given as $2e^{-(t-0.1T)/\tau}$ appears in the value for V_0 and $\dot{W}_R(6)$ when inhalation instead of exhalation is considered. Because this term assumes no definite value, the use of these equations for inhalation makes no more sense mathematically than it does physiologically.

When exhalation flow rate is limited, the exhalation muscle pressure is undetermined. Actual muscle pressure could theoretically assume any value in the range where flow rate becomes constant. For our purposes, maximum expiratory pressure was assumed to be applied. This gives the maximum rate of respiratory work. From data in Rahn *et al.* [17],

$$p_{max} = 4325.651 + 11703.94(V \text{ B RV})/\text{VC} \tag{17}$$

where

p_{max} is the maximum expiratory pressure (N/m^2),
VC is the vital capacity (m^3).

The value for p_{max} includes both muscle pressure and lung recoil pressure.

Respiratory rate of work was calculated from:

$$\dot{W}_R(6) = \frac{1}{T}\int_0^T p_{max}\dot{V}_L\,dt \tag{18}$$

where

$\dot{W}_R(6)$ is the average respiratory work rate during flow limitation (N m/s),
T is the duration of waveform (s),
t is the time (s).

Expressions for calculations of the different components of respiratory work rate for the flow limited hybrid exponential waveform appear in Table 7. Contributing to the total work rate are components previously obtained for the same waveform during the linear rise and fall phases in the time intervals $0 \le t \le 0.1T$ and $0.9T \le t < T$. However, as seen in Table 8, the work rate contribution during the limited flow phase is very high. The plain hybrid exponential waveform components are included as a comparison. Initial volumes for the two are nearly identical.

Table 7.
Average work rate components for the limited-flow hybrid exponential waveshape

$\dot{W}_R(1) = \frac{K_1\dot{V}_{max}^2}{30}(1 + e^{-1.6T/\tau})$
$\dot{W}_R(2) = \frac{K_2\dot{V}_{max}^3}{40}(1 + e^{-2.4T/\tau})$
$\dot{W}_R(3,1) = 2 - 2S\tan^{-1}(1/S) \qquad S^2 > 0$
$\dot{W}_R(3,1) = -2 + S\log\left(\frac{S+1}{S-1}\right) \qquad S^2 < 0$
$S = \frac{\sqrt{20V_0}}{\dot{V}_{max}T}$

Table 7.
(Continued)

$$\dot{W}_R(3,3) = \frac{2}{r}\left(\mp 100e^{-1.6T/\tau} - 20ae^{-0.8T/\tau}\right)\tan^{-1}\left(\frac{e^{-0.8T/\tau}}{r}\right) \mp 2e^{-0.8T/\tau} \qquad r^2 > 0$$

$$\dot{W}_R(3,3) = \left(100e^{-1.6T/\tau} \pm 20ae^{-0.8T/\tau}\right)\frac{L_6}{r} \mp 2e^{-0.8T/\tau} \qquad r^2 < 0$$

$$r = \sqrt{\mp 20ae^{-0.8T/\tau} - 100e^{-1.6T/\tau}}$$

$$a = \frac{V_0}{\dot{V}_{max}T} \pm 0.05 \pm \frac{\tau}{T}(1 - e^{-0.8T/\tau}) \mp 4.95e^{-0.8T/\tau}$$

$$L_6 = \pm \log\left[\frac{r + e^{-0.8T/\tau}}{r - e^{-0.8T/\tau}}\right]$$

$$\dot{W}_R(3) = \frac{K_3\dot{V}_{max}}{T}\left(\dot{W}_R(3,1) + \dot{W}_R(3,3)\right)$$

$$\dot{W}_R(4) = \frac{\dot{V}_{max}^2 T}{20C}\left[\frac{1}{40} + \frac{e^{-0.8T/\tau}}{20} + \frac{e^{-1.6T/\tau}}{40} + \frac{\tau e^{-0.8T/\tau}}{T}(1 - e^{-0.8T/\tau})\right]$$

$$- \frac{(V_0 - V_r)(0.05T\dot{V}_{max})(1 + e^{-0.8T/\tau})}{CT}$$

$$\dot{W}_R(5) = \pm\frac{I\dot{V}_{max}^2}{2T}(1 - e^{1.6T/\tau})$$

$$\dot{W}_R(6) = \frac{\dot{V}_{max}\tau}{T}\left[4325.651(1 - e^{-0.8T/\tau}) \mp \frac{11703.94}{2VC}\tau\dot{V}_{max}(1 - e^{-1.6T/\tau})\right]$$

Table 8.
Contributions of different components (N m/s) to exhalation work rate for the hybrid exponential and limited-flow hybrid exponential waveshapes during heavy exercise

	Hybrid exponential	Limited-flow hybrid exponential
$\dot{W}_R(1)$	2.86	0.340
$\dot{W}_R(2)$	0.313	0.0385
$\dot{W}_R(3)$	0.374	0.0349
$\dot{W}_R(4)$	−0.537	0.145
$\dot{W}_R(5)$	0	0.0467
$\dot{W}_R(6)$	–	17.2
Total	3.01	17.8
Initial volume (m^3)	3.67×10^{-3}	3.72×10^{-3}

Maximum flow rates are 5.34×10^{-3} m^3/s for both waveshapes; exhalation time = 0.75 s; minute volume = 1.33×10^{-3} m^3/s; tidal volume = 1.93×10^{-3} m^3; vital capacity = 0.0048 m^3; time constant = 0.412 s.

The limited-flow hybrid exponential waveform requires over seven times the power expended by the trapezoidal waveform appearing in Table 6. For very heavy exercise conditions, where limited flow is more likely to appear, total waveform work rate is 29.4 N m/s.

7. RESPIRATION AS AN ADDITIONAL METABOLIC BURDEN

Work done by the respiratory muscles uses oxygen and requires additional respiratory ventilation to support it. The respiratory muscles are about 10% efficient [2], thus leading to 10 N m/s physiological work for each 1 N m/s respiratory work. Each 1 N m/s of physiological work requires about 4.96 x 10^{-6} m^3/s of oxygen consumption. The translation from oxygen consumption to minute ventilation requires knowledge about the oxygen demands of the exercise the person is performing.

Table 9.
Parameter values used for the comparison between respiratory waveforms when respiratory work caused additional oxygen consumption

	Oxygen consumption (m^3/s)	Percent maximum oxygen uptake	Inhalation time (s)	Exhalation time(s)
Component				
Rest	5×10^{-6}	9	1.5	3.0
Light	1×10^{-5}	18	1.25	2.0
Moderate	3.55×10^{-5}	6.5	1.0	1.1
Heavy	4.7×10^{-5}	85	0.70	0.75
Very heavy	4.79×10^{-5}	87	0.50	0.50

Maximum oxygen uptake = 5.5×10^{-5} m^3/s.

For this study, five work rates were chosen and typical oxygen consumption values [18] were assigned to each (Table 9). Total oxygen consumption ($\dot{V}_{O_2}$) was determined as the sum of the above oxygen consumption rates plus respiratory oxygen consumption. Minute ventilation was obtained from total oxygen consumption by the following equation fitted to data in Astrand and Rodahl [19] for a subject with maximum oxygen uptake of 5.5 x 10^{-5} m^3/s $\dot{V}_{O_2}$ (Fig. 6):

$$\dot{V}_{avg} = 22.3401\ \dot{V}_{O_2} + 2.557642 \times 10^{-5} \tag{19}$$

$$\dot{V}_{avg} = \dot{V}_{avg} - 1.095938 \times 10^{-4} + 3.196486 \times 10^{-9}/(5.5 \times 10^{-5} - \dot{V}_{O_2}) \quad \text{for } \dot{V}_{avg} > 2.58333 \times 10^{-5} \tag{20}$$

where

$\dot{V}_{O_2}$ is the oxygen consumption (m^3/s),
$\dot{V}_{avg}$ is the minute ventilation (m^3/s).

Mechanical properties of the respiratory system remained at previous values. Initial inspiratory and expiratory lung volumes, tidal volumes, and time constants were calculated for each specific minute ventilation value. Because of the nonlinear relationship between minute ventilation and oxygen consumption, minute ventilation values had to be obtained by iteration.

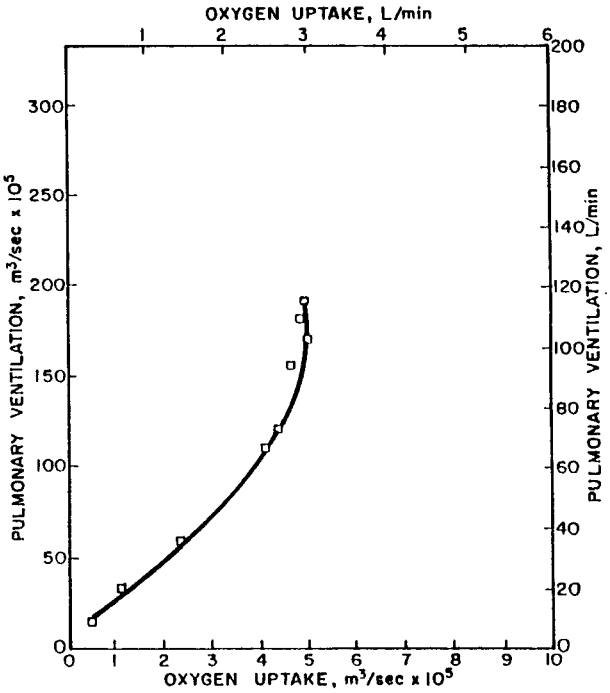

Figure 6. Pulmonary ventilation for various levels of oxygen consumption during rest and exercise for an individual with an anaerobic threshold of about 2.58×10^{-5} m^3/s oxygen consumption and a maximum oxygen uptake of 5.5×10^{-5} m^3/s.

Table 10.
Respiratory work rates (N m/s) for six different waveshapes when respiratory work rate poses an additional oxygen burden (expiratory values are in parentheses)

	Exercise level				
Waveshape	rest	light	moderate	heavy	very heavy
Sinusoidal	0.0886	0.231	2.22	54100[a]	47500[a]
	(0.0176)	(0.0674)	(1.13)	(3.62)	(6.15)
Rectangular	0.0727	0.186	1.83	5.68	5.75
	(0.0137)	(0.0521)	(0.833)	(2.61)	(3.87)
Trapezoidal	0.0779	0.199	1.97	6.51	7.83
	(0.0157)	(0.0582)	(0.936)	(2.97)	(4.42)
Truncated	0.145	0.322	2.68	38000[a]	32500[a]
exponential	(0.0618)	(0.157)	(1.56)	(3.74)	(4.57)
Hybrid	0.131	0.299	2.57	42300[a]	36400[a]
exponential	(0.0479)	(0.132)	(1.45)	(3.74)	(5.34)
Limited-flow	—	—	—	—	—
hybrid exponential	(0.747)	(1.69)	(10.3)	(21.1)	(26.8)

[a] Oxygen use exceeds maximum oxygen consumption. Oxygen debt is incurred.

Results appear in Table 10. Several features appear to be striking. First, at rest and light exercise, there is very little penalty to be paid for different respiratory waveshapes. Although the relative work rates vary considerably, absolute values for respiratory oxygen consumption are all less than 2% of the total. Minute volumes, tidal volumes, initial lung volumes and elastic work rates were found to be independent of waveshape, excluding the flow-limited hybrid exponential. In this region, too, exhalation work rates are very much less than inhalation work rates, probably because of the asymmetry in lung initial volumes between inhalation and exhalation.

For heavy and very heavy exercise levels, there was a clear distinction between waveshapes. Those that required more work also required more ventilation, and, because of the steep slope of the minute ventilation oxygen consumption curve, a severe penalty was paid for the higher oxygen requirement. Three of the waveshapes required higher oxygen consumptions than could be supplied for the inhaled breath. Oddly enough, the flow-limited hybrid exponential waveshape did not reach the maximum oxygen uptake point because of the energy advantage enjoyed during exhalation.

8. DISCUSSION AND CONCLUSIONS

The process of deriving expressions for respiratory work rate for different airflow waveforms was very tedious. Nevertheless, modelling that is needed to assist mask designers by accurately predicting the effects of respirator masks required the development of these expressions. Results appear to be confirmed by comparisons with other data, assuring that these expressions give at least partially valid results.

Along the way, an explanation was discovered for the change of lung initial volume during exercise. Other previous explanations were either unsatisfying or incorrect. The equal-pressure hypothesis appears to predict good results.

This study begged the question of determination of respiratory waveform. Others in the past had spent a great deal of effort trying to arrive at satisfactory waveform predictions. This study, on the other hand, assumed the waveforms and went on from there. Further work will be required to determine how and when respiratory waveforms change. Previous work will likely prove very valuable here.

This study has at least partially answered the question of why we breathe as we do. For this reason, I hope that it will have some value for those interested in physiological modelling of respiration.

REFERENCES

1. S. M. Yamashiro and F. S. Grodins. Optimal regulation of respiratory airflow. *J. Appl. Physiol.* **30**, 597-602 (1971).
2. A. T. Johnson. *Biomechanics and Exercise Physiology*. John Wiley, New York (1991).
3. R. P. Hämäläinen and A. A. Viljanen. Modeling the respiratory airflow pattern by optimization criteria. *Biol. Cybernet.* **29**, 143-149 (1978).
4. A. T. Johnson and C. Masaitis. Prediction of inhalation time exhalation time/ratio during exercise. *IEEE Trans.* **BME-23**, 376-380 (1976).
5. V. E. Ruttiman and W. S. Yamamoto. Respiratory airflow patterns that satisfy power and force criteria of optimality. *Ann. Biomed Eng.* **1**, 146-159 (1972).

6. A. T. Johnson. Conversion between plethysmograph and perturbational airways resistance measurements. *IEEE Trans.* **BME-33**, 803-806 (1986).
7. R. P. Hämäläinen and A. Sipilä. Optimal control of inspiratory airflow in breathing. *Optim. Control. Appl. Methods* **5**, 177-191 (1984).
8. A. T. Johnson and J. M. Milano. Relation between limiting exhalation flow rate and lung volume. *IEEE Trans.* **BME-34**, 257-258 (1987).
9. A. C. Jackson and K. R. Lutchen. Physiological basis for resonant frequencies in respiratory system impedances in dogs. *J. Appl. Physiol.* **70**, 1051-1056 (1991).
10. T. Kochi, J. H. T. Bates, S. Okubo, E. S. Petersen and J. Milic-Emili. Respiratory mechanics determined by flow interruption during passive expiration in cats. *Resp. Physiol.* **78**, 243-252 (1989).
11. S. M. Yamashiro and F. S. Grodins. Respiratory cycle optimization in exercise. *J. Appl. Physiol.* **35**, 522-525 (1973).
12. S. M. Yamashiro, J. A. Daubenspeck, T. N. Lauritsen and F. S. Grodins. Total work rate of breathing optimization in CO_2 inhalation and exercise. *J. Appl. Physiol.* **38**, 702-709 (1975).
13. A. T. Johnson. Multidimensional curve fitting program for biological data. *Comp. Prog. Biomed.* **18**, 259-264 (1984).
14. A. T. Johnson and H. M. Berlin. Exhalation time characterizing exhaustion while wearing respiratory protective masks. *J. Am. Ind. Hyg. Ass.* **35**, 463-467 (1974).
15. A. T. Johnson and A. V. Curtis. Minimum exhalation time with age, sex, and physical condition. *J. Am. Ind. Hyg. Ass.* **39**, 820-824 (1978).
16. A. Bouhuys, and B. Jonson. Alveolar pressure, airflow rate, and lung inflation in man. *J. Appl. Physiol.* **22**, 1086-1100 (1967).
17. H. Rahn, A. B. Otis, L. E. Chadwick and W. O. Fenn. The pressurevolume diagram of the thorax and lung. *Am. J. Physiol.* **146**, 161-178 (1946).
18. A. T. Johnson, R. A. Weiss and C. Grove. Respirator performance rating table for mask design. *J. Am. Ind. Hyg. Ass.* **53**, 193-202 (1992).
19. P.-O. Astrand and K. Rodahl. *Textbook of Work Physiology.* McGraw-Hill, New York (1970)

Frontiers Med. Biol. Engng, Vol. 4, No. 4, pp. 271-289 (1992)

ORIGINAL PAPER

Modelling exercise-induced pulmonary hemorrhage in racing thoroughbreds

ARTHUR T. JOHNSON,[1] LAWRENCE R. SOMA[2] and CARMELLA FEROUZ[3]

[1]*Agricultural Engineering Department, University of Maryland, College Park, MD 20742, USA*
[2]*New Bolton Veterinary Medicine Center, University of Pennsylvania, Kennett Square, PA 19348, USA*
[3]*Mechanical Engineering Department, University of Maryland, College Park, MD 20742, USA*

Received 14 October 1991; accepted 13 April 1992

Abstract-Exercise-induced pulmonary hemorrhage (EIPH) affects a large portion of racing thoroughbred horses. Sites of hemorrhage and causal mechanisms remain unestablished. Our mathematical model was constructed to test the hypothesis that EIPH could be caused by a combination of respiratory and circulatory mechanical factors occurring during exercise. Various physiological data for respiration, blood circulation and exercise were incorporated into the model. Results show that inhalation pressure drops across airway resistances become great enough during exercise to cause rupture of capillaries for both bronchial and pulmonary systems

Key words: horses; exercise; respiration; pulmonary system; capillary bursting.
Scientific Article Number A5091 Contribution Number 8151 of the Maryland Agricultural Experiment Station (Department of Agricultural Engineering).

1. INTRODUCTION

Among competitive race horses, it has been found that respiratory hemorrhage occurs in 44-75% of racing thoroughbreds [1]. Observed to occur after high levels of exercise, the phenomenon has come to be named exercise-induced pulmonary hemorrhage (EIPH).

There have been few studies done to determine the etiology and specific anatomic location of this bleeding, and there are many uncertainties and conflicting findings. Detection of EIPH in live horses is by examination of the upper airways with a fiber optic endoscope [1, 2]. The determination of the degree of EIPH is subjective and is dependent upon clearance of blood from the more peripheral portions of the lung to a central location where diagnosis can be made. Bronchoscopic examination is limited to diagnosis and not to hemorrhage location.

The location of EIPH incidence has only been determined with postmortem examination. Mason *et al.* [3] examined 117 horses and found that 96% had evidence of old alveolar hemorrhage and bronchiolitis. A full 82% of these horses showed signs of hemorrhage in the posterior lobes of the lung, the farthest areas from the bronchial entrances, and not distributed over either dorsal or ventral lung areas.

The cause of EIPH has also been debated. Early research attributed EIPH to obstructive disorders of the upper respiratory tract [4], while more recent research has suggested bronchiolitis and/or related neovascularization as possible causes [5]. Most significantly, however, it has been suggested that large pressure drops in the airways may be the cause of capillary rupture and hemorrhage into the lungs [4]. Along these same lines, transpulmonary pressure increases have been found to increase the likelihood

of tissue rupture and leakage in the lung [6].

The hypothesis suggested here is that high flow rates occurring during times of intense exercise result in high pressure drops across airways resistance and may cause airway or alveolar pressure to become low enough to cause blood vessel rupture. This model was constructed to determine if transmural strength of the pulmonary vasculature could be exceeded by mechanical factors during racing and to determine if further experimental investigation along this line is warranted.

2. THE **MODEL**

This model integrates respiratory, circulatory and exercise biomechanical concepts. Although each of these can be described somewhat independently, cross-references must be repeatedly made in order to completely describe the model.

The most difficult problem encountered when modeling this system was that of determining all the necessary numerical data. While values of airflow rates, heart rates, respiration rates and others have been separately measured for some exercise conditions [7, 8], we have been unable to locate a totally-integrated set of measurements. Values used in our analysis were assumed or estimated using the little information available from horses and sometimes from man.

2.1. Respiration

Our simple mathematical model of horse respiratory mechanics is shown in Fig. 1. Following the partitioning suggested by Robinson and Sorenson [4], respiratory airways .resistance has been segmented into upper airways (nares through pharynx), middle airways (pharynx through fifth generation bronchi) and lower airways (fifth generation bronchi to alveoli). Pressures have been calculated at the junction of middle and lower airways, and at the alveolar level. For the sake of simplicity, the bronchiolar circulation was placed at the junction of middle and lower airways, and the pulmonary circulation was placed at the alveolar level.

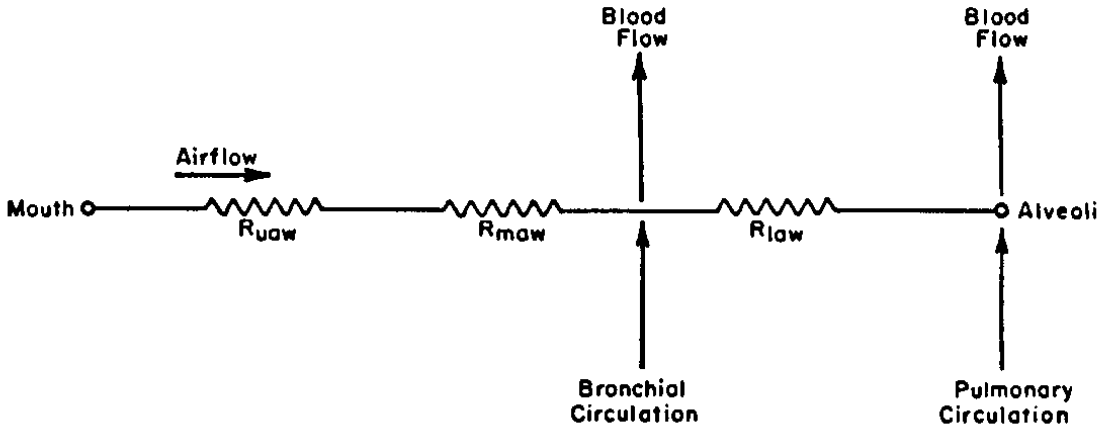

Figure 1. Diagram of the model used in this paper. Upper (nares to the trachea), middle (trachea to fifth bronchial generation) and lower (fifth generation to alveoli) segments comprise respiratory airways resistance. The bronchial circulation is assumed to be located between middle and lower resistance segments, whereas the pulmonary circulation is assumed to be located with the alveoli. The model compares air pressures and blood pressures with assumed bursting pressures of the arterioles and capillaries.

Other mechanical parameters were assumed to be unimportant for purposes of this model. Respiratory compliance is almost wholly due to elastic tissues. It is true that additional muscle pressure is necessary to overcome compliance, but this pressure is beyond the sites important to our model. Airway compliance, which is within the bounds of our model, is assumed to be so small to be negligible [9]. Art *et al*. [10] measured pulmonary inertance and respiratory inertance in ponies as 2.0 and 3.0 Pa s/l, respectively, and they asserted that inertance values were high enough to be a significant factor in limiting exercise ventilation. Inertance was not included in our model because we have made an assumption of a square-wave breathing pattern. Pressure losses due to inertance are only of significance during the rising and falling portions of the respiratory waveform and not during the constant flow rate periods where we had most interest. Therefore, only resistances appear in the model.

Consider first the upper airway resistance, R_{uaw} . This resistance is mainly due to the nasopharyngeal passages, and includes resistance created by the nares, the larynx and the turbinates [11]. Nasal resistance for the horse makes up only 10-19% of the total airway resistance [4]. Because of the high flow rates in the upper airways, we would have expected upper airways resistance to follow the Rohrer description:

$$R = K_1 + K_2 \dot{V} . \tag{1}$$

However, Derksen *et al.* [11] measured upper airway resistance and found it to be nearly constant with an average value of 0.378 cm H_2O-s/l over a range of now rates and exercise/rest conditions. They attributed this unexpectedly constant behavior to airway dilation with increasing airflow rates. It is possible that dilation does not occur over the full range of airflows for racing horses [12]. Nevertheless, upper airways resistance has been assumed to remain constant. The value of 0.378 cm H_2O-s/l is much too high, however, to yield realistic model results at high exercise levels.

Normal values for airway resistance in man vary around 1-2 cm H_2O-s/l. According to Spells [13], airways resistance should be reduced in larger animals according to the relationship:

$$R_{aw} \propto \text{mass}^{-0.862} \tag{2}$$

Using a human body mass of 70 kg and a horse body mass of 475 kg, total resting airway resistance should be no more than 0.69 cm H_2O-s/l for the horse. Twenty percent of this value has been assigned to upper airway resistance:

$$R_{uaw} = 0.140. \tag{3}$$

Middle and lower airways resistance constitute all remaining airways resistance. Thus, middle and lower airways resistances were assumed to represent 80% of total resistance. Middle airways resistance has been estimated to be 80% of the combined middle and lower airways resistance [4]. Middle airways resistance was thus taken to be 64% of total airways resistance [4] or 0.44 cm H_2O-s/l at an assumed travelling speed of 1.3 m/s.

Unlike upper airways, the middle, or cartilaginous, airways are unlikely to exhibit a constant resistance value. They are expected to obey Rohrer's description. Choice of K_1 and K_2 values are based on published human values [14, 151 with the body mass correction of equation (2) applied:

$$R_{maw} = 0.192 + 0.0192 \dot{V} . \tag{4}$$

Total area of the lower airway segment probably increases so much that turbulence is not usually considered a significant contributor to airway resistance [16]. However, it is here that distensible airways exhibit a resistance dependence on lung volume [17]. As the lung expands, the airways expand and resistance decreases.

Horses have very large lungs incompletely divided into lobes [7]. This allows gas to pass between adjacent regions through collateral pathways. The amount of collateral ventilation in normal horses is probably small because of long collateral time constants [7], most likely reflecting high resistance. It is unlikely, therefore, that differences in lung structure between horses and humans significantly influences the volume dependency of lower airway resistance.

Since blood vessel hemorrhaging would only likely occur because of vessel stretching or low airways or alveolar pressures, only lung volume during inspiration need be determined. It is likely that respiratory hemorrhage occurs when the lung is stretched its maximum amount, when R_{law} is at its minimum, but a reasonable argument could be made for using the maximum R_{law}, since this value would result in the most negative alveolar pressures. Thus, we have chosen to evaluate R_{law} at average inspiratory volume.

Unlike resting human breathing, horse resting breathing occurs around the equilibrium position, not above [7, 18]. Exercise inspiration begins at a volume lower than functional residual capacity (FRC) and at a point higher than the residual volume (RV). It has been shown in man that end-expiratory volume decreases during exercise [19, 20] and it is also likely that expiratory reserve volume (ERV) in horses declines as breathing becomes deeper in response to exercise demands. The relationship between this decline and other exercise parameters is not clear. The most reasonable approach, we have decided, is to assume that breathing in exercise continues to be centered about FRC, at least until RV is reached. FRC is taken to be the same as relaxation volume measured at rest.

FRC for the horse was assumed to be about 19 L. This was determined from an FRC constant of 40 ml/kg [21] and a body mass of about 475 kg.

Lower airways resistance was taken to be 16% of total airways resistance. Since average lung volume during inspiration is FRC (Fig. 2), R_{law} becomes independent of lung volume for our purpose. Thus,

$$R_{law} = 2.09/\mathrm{FRC} = 0.11 \tag{5}$$

The above equation would have been incorrect if calculated values for $V_T/2$ exceeded lung ERV. Because lung volume cannot be smaller than residual volume (Fig. 2), lower airway resistance would be calculated from:

$$R_{law} = 0.362/(\mathrm{RV} + V_T/2), \tag{6}$$

where RV is the residual volume, assumed to be 9 L [22]. As it turned out, tidal volumes never exceeded the limit (Table 2) where equation (6) was required to replace equation (5).

Minute volume (the product of tidal volume and respiration rate) has been assumed to vary linearly with locomotion speed [7, 23] until the anaerobic threshold is reached at a heart rate of 200 beats/min [24]:

$$\dot{V}_E = 200 + 120\ (\mathrm{speed}) \qquad 2.6 \leq \mathrm{speed} \leq 5.25 \tag{7}$$

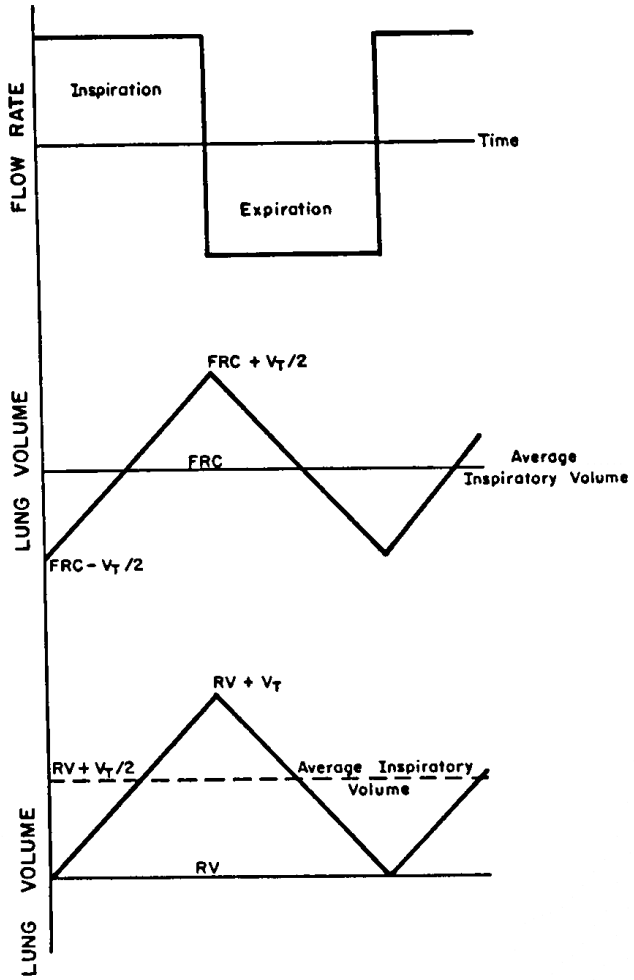

Figure 2. Assumed airflow rates are constant (upper plot). Lung volume with time is therefore a triangular shape centered around FRC (middle plot). During very heavy exercise, if $V_T/2$ exceeds ERV, lung volume with time becomes a triangular shape centered around $RV + V_T/2$ (lower plot).

Thereafter, minute volume was increased non-linearly in our model to account for the increased ventilation (Fig. 3):

$$\dot{V}_E = -119 + 120\ (\text{speed}) - 4632/(\text{speed} - 20.25) \qquad \text{speed} > 5.25. \tag{8}$$

Near rest, minute volume was calculated from

$$\dot{V}_E = 80.4 + 166\ (\text{speed}) \qquad \text{speed} < 2.6. \tag{9}$$

Respiratory rates were linearly related to oxygen consumption in man until the anaerobic threshold [25]. Thereafter, tidal volume became limited and respiratory rate increased disproportionately. Respiratory rates were assumed to vary linearly with oxygen consumption which, in turn, varied linearly with speed [26] for low horse locomotion speeds:

$$f = 4.05 + 29.19\ (\text{speed}) \qquad 1.3 \leq \text{speed} \leq 5, \tag{10}$$

where f is the respiratory rate (breaths/min).

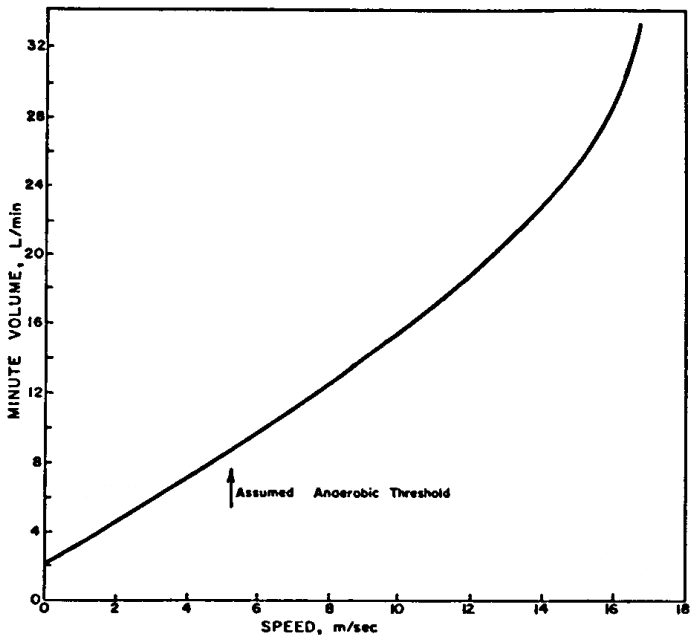

Figure 3. Assumed minute volume with racing speed. Speed was taken to be linearly related to work rate and the anaerobic threshold occurred at a heart rate of 200 beats/min.

Complicating the assignment of exercise respiration rates in our model is the apparent entrainment of respiration rate with gait in horses [27-29]. Bramble and Carrier report that breathing and gait could be tightly coupled in the trot, but that there was no apparent phase locking and breathing was sometimes erratic. They further asserted that breathing and gait were almost always coupled during the cantor and gallop. Synchronization occurs at one breath per stride.

Choosing appropriate respiration rates for our model therefore became enmeshed with determination of stride rates during heavy exercise. Bramble and Carrier [28] reported that stride frequency increased linearly with speed in the walk and trot, but remained essentially constant in the gallop. Nearly all gains in galloping speed resulted from longer stride, and, as a result, breathing rates became approximately fixed as the gallop began. Heglund *et al.* [30] also reported nearly constant galloping stride frequency. They gave an equation for stride frequency (sf) at the beginning of the gallop as:

$$\mathrm{sf} = 269\ \mathrm{M}^{-0.14}, \tag{11}$$

where *M* is the body mass (kg). For their 680 kg horse data, stride frequency became 108/min. This compares poorly to a maximum stride rate of 180/min given by Attenburrow [27].

Derksen *et al.* [11] provided respiration rates of 33, 62, 76 and 90 breaths/min for resting, walking, slow trotting and trotting conditions. Inspiratory flow rates for these same conditions were 5.0, 14.5, 30.0 and 40.1 l/s. These respiration rates appear to be too high in relation to other data. Koterba *et al.* [18] reported resting respiration rates of 6.2–21.3, with an average of 12.3 breaths/min for nine horses. Their corresponding average peak inspiratory flow rate was 3.56 l/s. Robinson [7] reported respiration rates of 80, 100 and 140 breaths/min for walking, cantering and galloping horses. Minute ventilation rates for these three conditions were 6.67, 13.33 and 23.33 l/s. Derksen *et al.* [11] reported that the highest peak

flow rate for exercising horses was approximately 57 l/s for a 475 kg horse at the fast gallop.

For our model we have chosen a resting respiration rate of 12/min, a trot-gallop respiration rate of 150/min and a maximum respiration rate of 180/min. Respiration rate was taken to be synchronized with stride rate during trotting and galloping, but not during walking. A small increase in stride frequency (and respiration rate) was allowed for the highest locomotion speed.

$$f = 137 + 2.56 \text{ (speed)} \qquad 5 < \text{speed}. \tag{12}$$

For the rest to walk transition,

$$f = 12 + 23.1 \text{ (speed)} \qquad \text{speed} < 1.3. \tag{13}$$

Tidal volumes were determined by dividing minute volumes by respiration rates in standard fashion:

$$V_T = \dot{V}_E / f. \tag{14}$$

Respiratory parameters in our model were based upon the assumption of constant inspiratory flow rate. Koterba *et al.* [18] have shown that inspiratory flow rate of a resting horse passes through two peaks with a shallow valley between. Inspiratory flow rate waveforms of running horses [12, 23] have shown that inspiratory flow rate is nearly constant.

Changes in respiratory patterns for exercising humans normally show the ratio of inspiratory time to expiratory time to increase as exercise progresses [31]. Whether or not this is true for exercising horses is entirely speculative. For convenience, we have assumed inspiration to occupy one-half of the respiratory period.

There was an error which accumulated because of the last two assumptions of constant flow rate and 50% inhalation time. Tidal volume calculated as one-half the product of peak flow rate and respiratory period appeared to be less accurate than using a fraction between one-half and one-third, based on data presented by Koterba *et al.* [18] and others. Therefore, flow rate was calculated as:

$$\dot{V}_{peak} = 2.61 V_T f, \tag{15}$$

where f is the respiration rate.

All respiratory pressures were calculated for inspiration only because mechanical rupture of surrounding blood vessels will occur for negative airway pressures. Since lung volume during the breathing period is cyclic, stretching, also thought to be related to hemorrhage, would be equally present during inhalation and exhalation.

2.2 *Circulation*

The vascular portion of the model required estimation of arteriole and capillary blood pressures for both pulmonary and bronchial circulation. Arterioles were considered because they are able to deliver

relatively larger quantities of blood to the hemorrhage site and capillaries were considered because of their relatively weak wall structure. Each of these pressures had to be obtained somewhat indirectly, since very little data was found that applied to the horse. Values from man were used as a guide, but blood pressure should be independent of body size [19].

Benekin and De Wit [32] gave capillary pressures to be related to arterial and venous pressures (in mm Hg):

$$p_c = 0.2p_a + 0.8p_v. \tag{16}$$

Therefore, pulmonary and bronchial arteriolar and venous pressures must be estimated.

Evans [33] has presented a compilation of blood systemic pressures in the horse at rest and during various forms of exercise. Values of systolic arterial pressures vary considerably, however. A resting systolic arterial pressure of 115 mm Hg was chosen as most reasonable. Significant increases in systolic arterial pressure occur during exercise and 205 mm Hg was reported at a galloping speed of about 10 m/s [33].

Assignment of pressure values to various points in the systemic circulation used human data as a guide. Johnson [9] gave resting systolic blood pressures in the human of 120, 70 and 30 mm Hg in the aorta, arterioles and capillaries. Aortic systolic pressure increases to 175 mm Hg during exercise. We have not found similar pressure values for exercise.

We know that blood pressure is influenced by cardiac output and vascular resistance. Without firm data upon which to base our assignment of pressure values, we have assumed no difference in systemic vascular resistance as it relates to the bronchial circulation. Thus, blood pressure changes during exercise largely as a result of increased cardiac output, which is itself a product of the stroke volume and heart rate.

Using available data [9] as a guide, systemic (bronchial) arteriolar pressures were calculated from:

$$p_{a_{syst}} = 66.02 + 0.16\ \mathrm{CO}, \tag{17}$$

where $p_{a_{syst}}$ is the systemic arteriolar pressure (mm Hg) and CO is the cardiac output (l/min).

Venous pressure was assumed to be related to venous return, which is related to stroke volume:

$$p_{v_{syst}} = 10.89 - 10.99\ \mathrm{SV}. \tag{18}$$

where SV is the stroke volume (l).

Pulmonary blood pressures were assigned in a manner similar to the systemic pressures. Johnson [9] gave human resting systolic blood pressures to be 25 mm Hg in the pulmonary artery and 10 mm Hg in the pulmonary capillaries. In addition, Spector [34] gave human pulmonary arterial pressures of 20, 35 and 50 mm Hg for the conditions of rest, moderate exercise and maximum work. Evans [33] gave resting pulmonary arterial systolic blood pressure in the horse as 42 mm Hg, which doubled during exercise. Robinson [7] gave similar figures.

Pulmonary arteriolar pressures should be significantly lower than systemic arteriolar pressures, and have been calculated from:

$$p_{a_{pulm}} = 35.28 + 0.188\ \mathrm{CO}. \tag{19}$$

Pulmonary venous pressures have been calculated to be higher than systemic venous pressures since the return vessels for the left atrium are considerably smaller than similar vessels for the right atrium:

$$p_{v_{pulm}} = 10.42 - 8.24 \text{ SV}. \tag{20}$$

It is known from humans [19] that heart rate is linearly related to oxygen consumption. The horse undergoes two locomotive transitions, from walking to trotting, and from trotting to galloping, each time becoming more efficient than if the transitions did not occur [35]. Hoyt and Taylor [36] have shown that the result of these transitions is that the oxygen cost to travel a given distance remains constant. Thus, oxygen consumption is linearly related to speed [26].

We have assumed heart rate to be directly related to speed up to maximum heart rate. We have assumed a maximum heart rate of 250 beats/min [24] and have maintained heart rate at maximum for higher speeds:

$$\text{hr} = 45 + 5.38 \text{ speed} \qquad \text{speed} < 1.3 \tag{21}$$
$$\text{hr} = 4.6 + 36.7 \text{ speed} \qquad 1.3 \leq \text{speed} < 5.5 \tag{22}$$
$$\text{hr} = 140.6 + 11.9 \text{ speed} \qquad 5.5 \leq \text{speed} < 9.2 \tag{23}$$
$$\text{hr} = 250 \qquad 9.2 \leq \text{speed}. \tag{24}$$

Stroke volume is known in humans to increase with exercise from 50% of maximum at rest up to 100% of maximum at 40% of maximum oxygen uptake [19]. Thereafter it remains at its maximum value until very severe exercise when atrial filling is insufficient to maintain stroke volume.

Resting stroke volume for the horse was determined from the allometric relationship [37]:

$$\text{SV} = (0.00078)M^{1.06}, \tag{25}$$

where SV is the stroke volume (l) and M is the mass (kg). Average mass of the horse was taken from Derksen *et al.* [11] to be 475 kg. We increased stroke volume in our model until an exercise heart rate of 200 was reached. It was at this level that Evans and Rose [24] suggested the anaerobic threshold was reached.

We have found other reports which again show the extreme variability of data from the horse. Evans [33] reported that stroke volume does not change significantly during exercise and its value remains at about 900 ml. Robinson [7] reported that cardiac output increases 5- to 8-fold during exercise and Wagner *et al.* [26] showed a 6-fold increase. Since heart rate increased no more than 4-fold, stroke volume must show some increase.

Stroke volumes were calculated from:

$$\text{SV} = 0.00078\, M^{1.06} + 0.049 \text{ (speed)} \qquad \text{speed} < 1.\ 3 \tag{26}$$
$$\text{SV} = 0.507 + 0.0714 \text{ (speed)} \qquad 1.3 \leq \text{speed} < 5.25 \tag{27}$$
$$\text{SV} = 0.9 \qquad 5.25 \leq \text{speed}. \tag{28}$$

Cardiac output was calculated in the traditional way:

$$\text{CO} = (\text{hr})\ (\text{SV}). \tag{29}$$

One possible reason for a difference between human and horse pulmonary circulatory pressures is the size of horse lungs. The most dorsal region of the horse lung is 30 cm above its heart; the most ventral region is 20 cm below its heart [7]. Such a difference would cause an almost 37 mm Hg vertical pressure gradient in the pulmonary circulation from top to bottom. It seems reasonable that ventral regions of the horse lungs would be the first to hemorrhage, but data in Mason *et al.* [3] shows the posterior regions to be the most likely to bleed. Since anterior lung regions did not indicate bleeding, the dorsal to ventral hydrostatic pressure gradient does not seem to be an important factor in EIPH. We have not included any blood pressure additions in our model to account for the gradient.

Capillaries may be very distensible and able to transmit external pressure differences to the inside by expansion. It is possible, however, that at the alveolar-capillary pressure differences present at high speeds, the ability of the capillaries to stretch further diminishes and compliance approaches zero [38, 39]. Pulmonary capillary compliance has not been measured in the horse to our knowledge. Therefore, we have included in our model the assumption that capillary compliance remains constant. A simplified diagram of the arterial, capillary and venous system is shown in Fig. 4. The capillary compliance connects the capillary interior with the airway or alveolus. Connecting the capillary compliance with the mean blood pressure source is a resistance located mainly in the arteriole. Connecting the capillary compliance with the venous compliance is a resistance located mainly in the capillary.

When pressure external to the capillary changes, the change is immediately transmitted to the capillary interior. As long as external pressure remains constant, internal pressure follows an exponential curve toward mean capillary pressure. During this time, the capillary is receiving more or less blood from the mean blood pressure source through the supply resistance. Time constant for this decay is the product of source resistance and capillary compliance.

If the time constant is very small, with respect to inhalation and exhalation times, then the decay is almost immediate and the pressure difference across the capillary wall becomes the difference between mean capillary pressure and alveolar or airway pressure. If the time constant is extremely long, then interior pressure remains at nearly mean capillary pressure minus alveolar or airway pressure, and the pressure difference across the capillary wall is just mean capillary pressure.

Measurements reported by Slife *et al.* [40] indicate that the time constant is about 0.4 s or intermediate between the two extremes, and of the same order of magnitude as inhalation time and exhalation time at

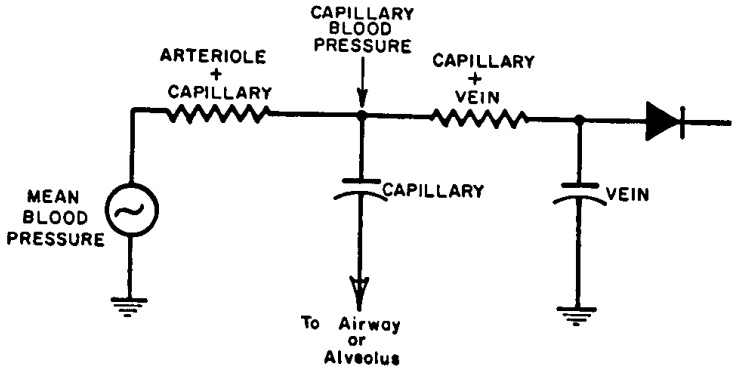

Figure 4. Simplified model of capillary compliance effects.

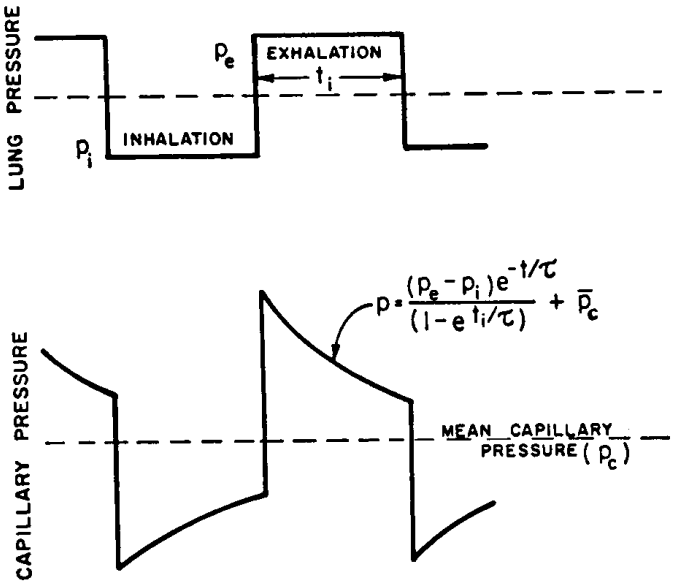

Figure 5. Time variations of lung intraluminal pressures as they affect capillary blood pressures.

the highest running speeds. We assumed equal inhalation and exhalation times, and equal pressure excursions in the respiratory system during inhalation and exhalation (Fig. 5). Therefore, capillary interior pressure became:

$$p_c = \frac{2p_a \exp(-t/\tau)}{(1 - \exp(-t_i/\tau))} + \bar{p}_c, \tag{30}$$

where $\bar{p}_c$ is the mean capillary pressure (mm Hg), p_a is the alveolar or airway pressure (mm Hg), t_i is the inhalation time (s) and τ is the time constant (s). The average capillary transmural pressure during inspiration is:

$$\overline{(p_c - p_a)} = -p_a + \frac{1}{t_i}\int_0^{t_i} p_c\, dt, \tag{31}$$

which became:

$$\begin{aligned}\overline{(p_c - p_a)} &= 2p_a\left(\frac{\tau}{t_i}\right) + \bar{p}_c - p_a \\ &= 2p_a(2\tau f) + \bar{p}_c - p_a.\end{aligned} \tag{32}$$

We used a value for $\tau = 0.4$ s for capillaries and r = 0 s for arterioles.

Bursting pressures of the various blood vessels in the respiratory system have not been measured to our knowledge. Prediletto *et al.* [41] reported that capillary rupture in rabbit lungs occurs over a range of pressures with higher numbers of ruptures at higher pressures. They reported no endothelial or epithelial breaks at 12.5 cm H_2O pressure, 10.8 endothelial and 10.2 epithelial breaks/mm at 52.5 cm H_2O pressure, and 39.8 endothelial and 6.7 epithelial breaks/mm at 72.5 cm H_2O. There was a large variability between animals and some evidence of structural damage clustering near supplying arterioles.

Burton [42] suggested that bursting of human arteries might occur at 200 mm Hg or at pressures roughly equal to twice the mean pressure. In scaling this pressure, we considered vessel radius, wall thickness and wall tissue. The law of Laplace:

$$p = \tau \Delta r / r, \tag{33}$$

shows that pressure inside a cylindrical tube can be calculated from wall shear stress (τ), wall thickness (Δr) and vessel radius (r). Tubes of smaller radius can contain higher pressures for the same wall shear. Bursting pressures were thus increased for smaller vessels.

These vessels were assumed to possess thin enough walls that bursting pressure was proportional to wall thickness. Also, capillary wall composition, consisting exclusively of endothelial tissue, should be weaker than artery and arteriole walls composed of endothelium, elastic tissue, muscle fibers, and fibrous tissue. These considerations are summarized in Table 1.

Table 1.
Comparison between systemic blood vessels of various sizes (data from Burton [42])

	Lumen diameter (mm)	Wall thickness (mm)	Wall material (relative amounts)				Assumed bursting pressure (mm Hg)
			end.	ela.	mus.	fib.	
Medium artery	4	1	1	10	14	4	200
Arteriole	0.03	0.02	1	5	11	4	500
Capillary	0.008	0.001	1	0	0	0	60

Bursting pressures for pulmonary arterioles and capillaries were assumed to be 400 and 48 mm Hg, respectively.

Pulmonary circulation pressures, derived from the right ventricle, are lower than systemic circulatory pressures. It is reasonable to expect bursting pressures in the pulmonary circulation to be lower than bursting pressures in the bronchial circulation. Pulmonary vessel bursting pressures were taken to be 0.8 those of systemic bursting pressures.

Exercise conditions which were used were based largely on data from Derksen *et al.* [11], which defined speeds, heart rates and respiratory flow rates for resting, walking, slow trotting and trotting. Values for these physiological parameters were extrapolated to a maximum speed of 16.7 m/s, which was the speed attained by *Secretariat* running the Belmont Stakes. Quasi-steady state was assumed for all physiological parameters at all speeds.

3. RESULTS

Results are found in Tables 2-4. Airway-blood vessel pressures were found to exceed bursting pressures in both systemic and pulmonary capillaries, and to nearly reach arteriole bursting pressures. Presumed bleeding occurs at lower running speeds in alveolar areas compared to bronchiolar areas, but the difference in speeds is very small.

Table 2.
Respiratory calculation results made with the mathematical model

Condition	Speed (m/s)	Peak flow (l/s)	Tidal volume (l)	Minute volume (l/min)	Respiration rate (min^{-1})	R_{uaw} (cm H_2O-s/l)	R_{maw} (cm H_2O-s/l)	R_{law} (cm H_2O-s/l)
Stand	0.0	3.5	6.7	80	12	0.140	0.26	0.110
Walk	1.3	12.9	7.1	296	42	0.140	0.44	0.110
Walk–trot transition	2.6	22.3	6.4	512	80	0.140	0.62	0.110
Slow trot	3.3	25.9	5.9	596	100	0.140	0.69	0.110
Trot	4.3	31.1	5.5	716	130	0.140	0.79	0.110
Trot–gallop transition	5.0	34.8	5.3	800	150	0.140	0.86	0.110
Anaerobic threshold	5.5	37.2	5.7	855	151	0.140	0.91	0.110
	7.5	49.8	7.3	1144	156	0.140	1.15	0.110
Fast gallop	9.2	61.1	8.7	1404	161	0.140	1.36	0.110
	10.0	66.7	9.4	1533	163	0.140	1.47	0.110
	12.0	81.9	11.2	1883	168	0.140	1.76	0.110
	14.0	100.1	13.3	2302	173	0.140	2.11	0.110
Racing	16.7	138.8	17.7	3190	180	0.140	2.86	0.110

Table 3.
Circulatory calculation results made with the mathematical model

Condition	Speed (m/s)	Heart rate (min^{-1})	Stroke volume (l)	Cardiac output (l/min)	Systematic artery pressure (mm Hg)	Systematic venous pressure (mm Hg)	Pulmonary artery pressure (mm Hg)	Pulmonary venous pressure (mm Hg)
Stand	0.0	45	0.536	24.1	70	5.0	39.8	6.0
Walk	1.3	52	0.600	31.3	71	4.3	41.2	5.5
Walk–trot transition	2.6	100	0.693	69.2	77	3.3	48.3	4.7
Slow trot	3.3	126	0.743	93.2	81	2.7	52.8	4.3
Trot	4.3	162	0.814	132.0	87	1.9	60.1	3.7
Trot–gallop transition	5.0	188	0.864	162.3	92	1.4	65.8	3.3
Anaerobic threshold	5.5	206	0.900	185.5	96	1.0	70.1	3.0
	7.5	230	0.900	206.9	99	1.0	74.2	3.0
Fast gallop	9.2	250	0.900	225.0	102	1.0	77.6	3.0
	10.0	250	0.900	225.0	102	1.0	77.6	3.0
	12.0	250	0.900	225.0	102	1.0	77.6	3.0
	14.0	250	0.900	225.0	102	1.0	77.6	3.0
Racing	16.7	250	0.900	225.0	102	1.0	77.6	3.0

Table 4.
Transmural calculation results made with the mathematical model

Condition	Speed (m/s)	Airway pressure (cm H_2O)	Airway-systemic artery presure difference (mm Hg)	Systemic capillary pressure (mm Hg)	Airway-systemic capillary pressure difference (mm Hg)	Alveolar pressure (cm H_2O)	Alveolar-pulmonary artery difference (mm Hg)	Pulmonary capillary pressure (mm Hg)	Alveolar-pulmonary capillary pressure difference (mm Hg)
Stand	0.0	−1.4	70.9	18.0	18.9	−1.8	41.1	12.8	13.9
Walk	1.3	−7.5	76.5	17.6	22.9	−8.9	47.7	12.6	18.9
Walk–trot transition	2.6	−16.9	89.5	18.0	30.2	−19.4	62.5	13.4	27.4
Slow trot	3.3	−21.5	96.8	18.4	33.9	−24.4	70.7	14.0	31.6
Trot	4.3	−29.0	108.4	19.0	40.0	−32.4	83.9	15.0	38.5
Trot–gallop transition	5.0	−34.8	117.6	19.5	44.8	−38.6	94.2	15.8	43.9
Anaerobic threshold	5.5	−38.9	124.3	19.9	48.2	−43.0	101.8	16.4	47.7
	7.5	−64.1	146.2	20.6	67.3*	−69.6	125.3	17.2	67.9*
Fast gallop	9.2	−91.9	169.6	21.2	88.1*	−98.6	150.1	17.9	89.7*
	10.0	−107.5	181.1	21.2	99.5*	−114.8	162.0	17.9	101.5*
	12.0	−155.9	216.6	21.2	134.7*	−164.9	198.8	17.9	138.0*
	14.0	−225.7	268.0	21.2	185.7*	−236.8	251.7	17.9	190.4*
Racing	16.7	−415.6	407.6	21.2	324.1*	−430.9	394.4	17.9	331.9*

*Hemorrhage occurs when intraluminal pressures and blood vessel pressures exceed assumed vessel bursting pressures.

Middle airways resistance dominates at high speeds because of its dependence on flow rate. Even if middle airways resistance were assumed constant at its resting value of 0.26 cm H_2O-s/l, bursting pressures in pulmonary capillaries would be exceeded for speeds in excess of 12 m/s and bursting pressures in bronchiolar capillaries would be exceeded for a speed of 16.7 m/s.

Although systemic arterial pressure is nearly twice pulmonary arterial pressure, systemic and pulmonary capillary pressures are not much different.

4. DISCUSSION

It was our intention with this model to demonstrate that EIPH could indeed be caused by low alveolar pressures occurring at the high flow rates generated by running horses. There is no doubt that the model succeeded in showing this fact.

We had also intended that the model would be simple and easy to follow. However, the physiology of exercising horses is not so simple and inclusion of as many physiological facts as were pertinent was also difficult. What has resulted is a model which is extremely reasonable and which agrees well with much published data. About the only model point which is somewhat questionable is the resting condition, because there was little agreement in the literature about conditions which prevail at rest. The careful reader will note discontinuities in trends for minute volume and respiration rate at the resting condition. What ameliorates this is that we are not too concerned about resting condition results.

This model essentially consists of a series of physiological facts and tendencies normally treated separately in the literature. That is, respiratory mechanics, exercise physiology and cardiovascular mechanics are usually not integrated to the extent of this model. Therefore, when the model did truly predict EIPH, a great confidence was felt that the physiological description was at least adequate.

It was not so surprising that we found EIPH to occur as a result of capillary rupture. Although the possibility of arteriolar rupture does exist, we really did not expect arteriolar bursting pressures to be exceeded. What was surprising is that there is very little difference in the speeds at which bronchial capillaries rupture and pulmonary capillaries rupture. Because of this, sources for EIPH must be very diffused and difficult to localize, a result confirmed by the literature.

A central question to ask with any model is how sensitive are the results to assumed values of parameters? There were many parameters with unknown values and a few that required assumed functional forms. Among the supposed values were those for upper, middle and lower airways resistance, minute ventilation, peak flow rate, inhalation/exhalation time ratio, capillary pressures, and bursting pressures. Sensitivity analyses of each of these would not only provide tedious reading, but would not yield a great deal of additional insight.

One way to combine many of these is to consider airways resistance multiplied by flow rate to be airways pressure drop. The ratio between upper airways and middle airways resistances would then be reflected as a ratio of pressure drops. Upper airways resistance and lower airways resistance are assumed for this analysis to remain related through a constant ratio, as in Table 2.

This sensitivity analysis appears in Fig. 6, which is a three-dimensional plot of upper airway pressure drop, the ratio of middle airway pressure drop to upper airway pressure drop and alveolar to capillary transmural pressure. When upper airway pressure drop is zero, the capillary transmural pressure becomes

equal to capillary blood pressure. For other upper airways pressure drops and other ratios, the graph becomes an inclined flat plane.

If airways resistance increases, the transmural pressure moves further up the plane. The same is true for increased respiratory flow rate. If capillary blood pressure increases or capillary compliance decreases, the entire plane becomes elevated more. Bursting pressure is a vertical level on the graph and where the inclined plane intersects this vertical level is the lowest value that bleeding begins. If bursting pressure increases, the critical vertical level of the plane moves higher.

The large negative airway and alveolar pressures encountered during extreme exercise (very few horses are capable of running at the 16.7 m/s speed) are determined largely by the values of R_{uaw}, R_{maw}, and R_{law} assumed in the model. We have tried to show that these assumed values are based on reasonable conclusions from published data. However, it is possible that one reason that a supreme racehorse like *Secretariat* could run as fast as he did was because he possessed airway resistances with values much lower than normal. This would lower his capillary transmural pressure on the plane in Fig. 6 and might avoid respiratory bleeding.

While Fig. 6 does not give numerical values for any of these parameters, it does convey the concepts of a sensitivity analysis. Since it is enough for the model to show that bursting is possible due to the mechanisms included in the model, we thought further sensitivity analysis to be unwarranted.

Middle airways resistance clearly dominates the airways pressure drop. With upper airways resistance being essentially constant and lower airways resistance to be inconsequential during inhalation, middle airways resistance is the main reason why EIPH occurs. We can speculate that a screening test given to

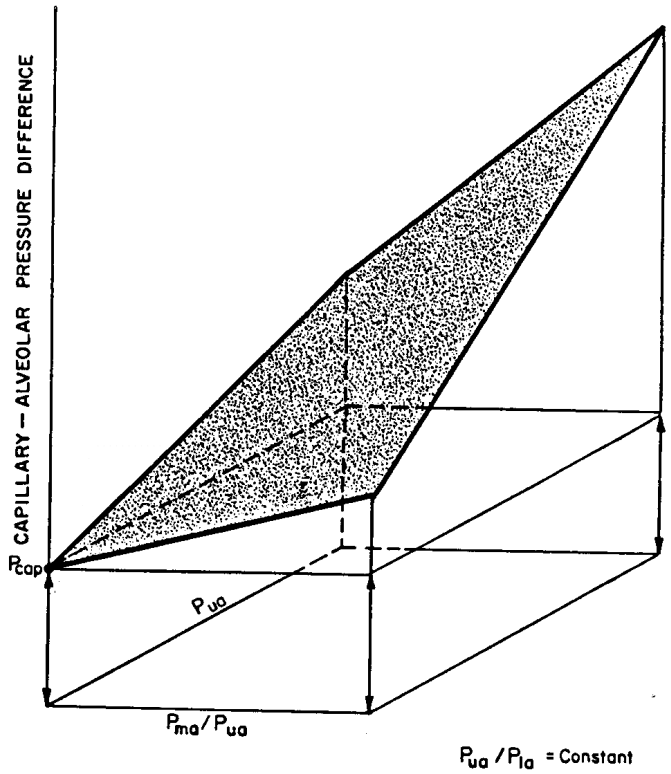

Figure 6. Sensitivity diagram for various model parameters with upper airway pressure to lower airway pressure ratio constant.

racehorses when they are young to determine the magnitude of airways resistance no further down than the fifth bronchiolar generation could be used to predict those which will be prone to EIPH. The lower the resistance, the less prone. Such a test may or may not correlate with bloodlines, but any potential buyer or trainer may have more than pedigree to consider when taking on a new thoroughbred.

We have been working for several years on a measuring instrument called the airflow perturbation device (APD) which could be the instrument of choice for this screening test [43]. It has the advantage of not requiring elaborate cooperation from the animal in order to make the measurement. A great deal of work needs to be accomplished, however, before we will be confident that a test made at rest will correlate with exercise conditions. If not, then the APD must be adapted to be used with running animals.

We have previously mentioned that published data from exercising horses often varies considerably. Some data is not available. Seemingly simple respiratory flow rate measurements are among these. It can be seen from our model that flow rates as high as 144 l/s can be expected from a horse running full out. Such a flow rate is incredible, being about 15-20 times the highest flow rates which we have measured on maximally exercising humans. It may be that such flow rates are not achieved in reality and that the horse running that fast must hypoventilate because sufficient intrapleural pressures cannot be achieved to propel air at such a rate. On the other hand, even flow rates half as high would be extremely difficult to measure, and there can be no wonder at the paucity of data in the literature.

Bursting pressures of blood vessels were not found in the literature. Most modern literature appears to dwell on the strengths of tissues subjected to surgery [44] or on bursting of large vessels undergoing angioplasty [45, 46] or on strengths of vascular prostheses [47]. Bursting pressures of large vessels were measured generally in excess of 1200 mm Hg, but these are not the values needed for this model. Physical properties such as these need to be measured, not only for EIPH studies, but also for studies involving cerebral hemorrhage, aneurisms, bleeding ulcers and others. We were surprised that such basic data were not at least easily located and intend that studies along this line would proceed in the near future.

REFERENCES

1. C. F. Raphel and L. R. Soma. Exercise-induced pulmonary hemorrhage in thoroughbreds after racing and breezing. *Am. J. Vet. Res.* **43**, 1123-1127 (1982).
2. J. R. Pascoe, A. E. McCabe, C. E. Franti and R. M. Arthur. Efficacy of furosemide in the treatment of exercise-induced pulmonary hemorrhage in thoroughbred racehorses. *Am. J. Vet. Res.* **46**, 2000-2003 (1985).
3. D. K. Mason, E. A. Collins and K. L. Watkins. Exercise-induced pulmonary hemorrhage in horses. In: *First Int. Symp. on Equine Exercise Physiology,* D. Snow (Ed.), 57-63. Burlington Press, Cambridge, UK (1982).
4. N. F- Robinson and P. R. Sorenson. Pathophysiology of airway obstruction in horses: a review. J. *Am. Vet. Med. Assoc.* **172**, 299-303 (1978).
5. M. W. O'Callaghan, J. R. Pascoe and W. S. Tyler. Exercise-induced pulmonary hemorrhage in the horse: results of a detailed clinical, post mortem and imaging study. V. Microscopic observations. *Equine Vet. J.* **19**, 411-418 (1987).
6. F. G. Hoppin, Jr and J. Hilderbrandt. Mechanical properties of the lung. In: *Bioengineering Aspects of the Lung,* J. B. West (Ed.), 83-162. Dekker, New York (1977).

7. N. F- Robinson. Respiratory adaptations to exercise. In: *Veterinary Clinics of North America: Equine Practice,* R. J. Rose (Ed.), 497-512. W. B. Saunders, Philadelphia (1985).
8. J. R. Thornton. Exercise testing. In: *Veterinary Clinics of North America: Equine Practice,* R. J. Rose (Ed.), 573-595. W. B. Saunders, Philadelphia (1985).
9. A. T. Johnson. *Biomechanics and Exercise Physiology.* Wiley, New York (1991).
10. T. Art, P. Lekeux, P. Gustin, D. Desmecht, H. Amory and M. Paiva. Inertance of the respiratory system in ponies. *J. AppL PhysioL* **67**, 534-540 (1989).
11. F. J. Derksen, J. A. Stick, E. A. Scott, N. E. Robinson and R. F. Slocombe. Effect of laryngeal hemiplegia and laryngoplasty on airway flow mechanics in exercising horses. *Am. J. Vet Res.* **47**, 16-20 (1986).
12. T. Art, D. Serteyn and P. Lekeux. Effect of exercise on the partitioning of equine respiratory resistance. *Equine Vet. J.* **20**, 268-273 (1988).
13. K. E. Spells. Comparative studies on lung mechanics based on a survey of literature data. *Resp. Physiol.* **8**, 37-57 (1969).
14. B. G. Ferris, J. Mead and L. H. Opie. Partitioning of respiratory flow resistance in man. *J. Appl. Physiol*. **19**, 653-658 (1964).
15. J. Mead and J. L. Whittenberger. Physical properties of human lungs measured during spontaneous respiration. *J. Appl. Physiol.* **5**, 779-796 (1953).
16. N. C. Staub. The interdependence of pulmonary structure. and function. *Anesthesiology* **24**, 831-854 (1963).
17. W. A. Briscoe and A. B. Du Bois. The relationship between airway resistance, airway conductance, and lung volume in subjects of different age and body size. *J. Clin. Invest.* **37**, 1279-1285 (1958).
18. A. M. Koterba, P. C. Kosch, J. Beech and T. Whitlock. Breathing strategy of the adult horse (Equus *caballus)* at rest. *J. Appl. Physiol.* **64**, 337-346 (1988).
19. P.-O. Astrand and K. Rodahl. *Textbook of Work Physiology.* McGraw-Hill, New York (1970).
20. S. M. Yamashiro. and F. S. Grodins. Respiratory cycle optimization in exercise. *J. Appl. Physiol.* **35***,* 522-525 (1973).
21. L. R. Soma, J. Beech and N. H. Gerber, Jr. Effects of cromolyn in horses with chronic obstructive pulmonary disease. *Vet. Res. Commun.* **11***,* 339-351 (1987).
22. P. R. Sorenson and N. E. Robinson. Postural effects on lung volumes and asynchronous ventilation in anesthetized horses. *J. Appl. Physiol.* **48**, 97-103 (1980).
23. A. J. Woakes, P. J. Butler and D. H. Snow. The measurement of respiratory airflow in exercising horses. In: *Equine Exercise Physiology 2,* J. R. Gillespie and N. E. Robinson (Eds), 194-205. ICEEP Publications, Davis, CA (1987).
24. E. L. Evans and R. J. Rose. Method of investigation of the accuracy of four digitally-displaying heart rate meters suitable for use in the exercising horse. *Equine Vet. J.* **18**, 129-132 (1986).
25. B. J. Martin and J. V. Weil. CO_2 and exercise tidal volume. *J. Appl. Physiol.* **46**, 322-325 (1979).
26. P. D. Wagner, J. R. Gillespie, G. L. Landgren, M. R. Fedde, B. W. Jones, R. M. De Bowes, R. L. Pieschl and H. H. Erickson. Mechanism of exercise-induced hypoxemia in horses. *J. Appl. Physiol.* **66**, 1227- 1233 (1989).
27. D. P. Attenburrow. Time relationship between the respiratory cycle and limb cycle in the horse. *Equine Vet. J.* **14**, 69-72 (1982).
28. D. M. Bramble and D. R. Carrier. Running and breathing in mammals. *Science* **219**, 251-256 (1983).
29. G. Dalin and L. B. Jeffcott. Locomotion and gait analysis. In: *Veterinary Clinics of North America: Equine Practice,* R. J. Rose (Ed.), 549-572. W. B. Saunders, Philadelphia (1985).
30. N. C. Heglund and C. R. Taylor. Scaling stride frequency and gait to animal size: mice to horses. *Science* **186**, 1112-1113 (1974).
31. A. T. Johnson. Effects of physical stress on the respiratory system. In: *Proc. Nat. Inst. Farm Safety,* General Session IV, 10-18 (1984).
32. J. E. W. Beneken and B. De Wit. A physical approach to hemodynamic aspects of the human

cardiovascular system. In: *Physical Bases of Circulatory Transport: Regulation and Exchange,* E. B. Reeve and A. C. Guyton (Eds), 1-45. W. B. Saunders, Philadelphia (1967).